Self-avoiding walk enumeration via the lace expansion

Nathan Clisby[1], **Richard Liang**[2] **and Gordon Slade**[3]

[1]ARC Centre of Excellence for Mathematics and Statistics of Complex Systems, Department of Mathematics and Statistics,
The University of Melbourne, Victoria 3010, Australia

[2]Department of Statistics, University of California, Berkeley, CA 94720-3860, USA

[3]Department of Mathematics, University of British Columbia, Vancouver, BC, Canada V6T 1Z2

E-mail: `N.Clisby@ms.unimelb.edu.au`, `rhliang@stat.berkeley.edu` and `slade@math.ubc.ca`

Abstract. We introduce a new method for the enumeration of self-avoiding walks based on the lace expansion. We also introduce an algorithmic improvement, called the two-step method, for self-avoiding walk enumeration problems. We obtain significant extensions of existing series on the cubic and hypercubic lattices in all dimensions $d \geq 3$: we enumerate 32-step self-avoiding polygons in $d = 3$, 26-step self-avoiding polygons in $d = 4$, 30-step self-avoiding walks in $d = 3$, and 24-step self-avoiding walks and polygons in *all* dimensions $d \geq 4$. We analyze these series to obtain estimates for the connective constant and various critical exponents and amplitudes in dimensions $3 \leq d \leq 8$. We also provide major extensions of $1/d$ expansions for the connective constant and for two critical amplitudes.

PACS numbers: 02.10.Ox, 05.10.-a, 05.50.+q, 05.70.Jk

July 24, 2007

1. Introduction and results

1.1. Introduction

The self-avoiding walk (SAW) is a fundamental model in combinatorics and statistical physics [48]. Efforts to enumerate SAWs have been undertaken during the last half century, starting with [16]. The continuing advance of computing hardware is certainly helpful to this endeavor, but the exponential complexity of the enumeration problem makes algorithmic advances just as important. On the square lattice $\mathbb{Z}^2$, the development of the finite lattice method (see [11]) has made it possible to enumerate SAWs up to and including 71 steps [41], and self-avoiding polygons up to 110 steps [40], a remarkable achievement. Above $d = 2$, progress has been less dramatic due to the lack of an efficient algorithm. On the cubic lattice $\mathbb{Z}^3$, SAWs have been enumerated up to and including 26 steps [47] (extending results of [25, 27, 46]), whereas enumerations in dimensions $d = 4, 5, 6$ are limited to respectively $19, 15, 14$ steps [8] (slightly extending results of [46]).†

In this paper, we propose and develop a new method for the enumeration of SAWs based on the lace expansion [4]. The lace expansion is a method that has been used in the mathematical literature to prove theorems about the critical behavior of SAWs, lattice trees and lattice animals, percolation, and related models, above their upper critical dimensions. For a recent overview, see [59]. In the case of SAWs, the lace expansion gives an identity involving the number of n-step SAWs, valid in all dimensions $d \geq 1$. The principal advantage of this identity, for enumeration purposes, is that it expresses the number of self-avoiding walks of length n in terms of the number of *lace graphs*. Lace graphs consist of self-avoiding polygons and certain related walk trajectories with self-intersections, taking n or fewer steps. These trajectories are less spatially extended than SAWs of the same length, and are hence less numerous, by a factor which is asymptotically the length to some non-negative power. This makes them easier to enumerate. In practice, for the square lattice there are approximately 36 times as many 30 step SAWs as there are lace graphs, while for the cubic lattice there are approximately 525 times as many SAWs of 30 steps as compared to lace graphs. This factor gets much larger as the dimension is increased: the factor for $d = 4$, $n = 24$ is approximately 1700, for $d = 5$, $n = 24$, it is approximately 6200, while for $d = 6$, $n = 24$, it is approximately 20000.

We also introduce an innovation for the direct enumeration of self-avoiding walks and polygons that we call the *two-step method*. This method provides an exponential improvement on brute force enumeration. We use the two-step method to enumerate the lace graphs, and the combination of the two-step method with the lace expansion proves to be quite effective.

† A note added in proof to [46] reports enumeration of SAWs up to 21 steps for $d = 4$ but does not reveal the number.

1.2. Enumeration results

An n-step SAW on $\mathbb{Z}^d$ is a mapping $\omega : \{0, 1, \ldots, n\} \to \mathbb{Z}^d$ with $|\omega(i+1) - \omega(i)| = 1$ for each i ($|x|$ denotes the Euclidean norm of x), and with $\omega(i) \neq \omega(j)$ for all $i \neq j$. For $x \in \mathbb{Z}^d$, let $c_n(x)$ denote the number of n-step SAWs on $\mathbb{Z}^d$ with $\omega(0) = 0$ and $\omega(n) = x$. Let $c_n = \sum_{x \in \mathbb{Z}^d} c_n(x)$ denote the number of n-step SAWs which start at 0, and let $\rho_n = \sum_{x \in \mathbb{Z}^d} |x|^2 c_n(x)$, so that $\bar{\rho}_n = \rho_n c_n^{-1}$ is the mean-square displacement. Let p_n denote the number of unrooted undirected self-avoiding polygons (SAP) of length n, i.e., $p_n = \frac{1}{2n} c_{n-1}(e)$ where e denotes a neighbor of 0 in $\mathbb{Z}^d$.

We used the two-step method to enumerate p_n for $n \leq 32$ for $d = 3$, for $n \leq 26$ for $d = 4$, and for $n \leq 24$ for *all* $d \geq 5$ (knowledge of p_n for $n \leq 24$ and $d \leq 12$ determines p_n also for $d > 12$ since polygons with at most 24 steps can occupy at most 12 dimensions). We have used the lace expansion to enumerate c_n and ρ_n for $n \leq 30$ for $d = 3$, and for $n \leq 24$ for *all* $d \geq 4$ — in fact the lace expansion shows that enumeration of c_n for $n \leq 2k$ and $d \leq k$ actually gives the enumeration of c_n for $n \leq 2k$ for *all* d, so it suffices to enumerate c_n for $n \leq 24$ and $d \leq 12$ here. Tables of these enumerations of p_n, c_n and ρ_n are given in Appendix A (see also [9]). In particular, for $d = 3$,

$$c_{30} = 270\,569\,905\,525\,454\,674\,614, \qquad p_{32} = 53\,424\,552\,150\,523\,386.$$

These enumerations are based on the enumeration of the lace graphs discussed in Section 3 below. Complete tables of the latter, also in machine-readable form, can be found in [9]. Our method also applies for $d = 2$, but does not compete with the finite lattice method [40, 41]. Our SAP enumerations differ from and correct those of [60] for $n = 18$ in dimensions $d = 4, 5, 6, 7$.

The SAP enumerations were performed on brecca, a Linux cluster of Xeon 2.8 GHz CPUs at the Victorian Partnership for Advanced Computing (VPAC). The $d = 3$, $n = 30$ calculation took 450 CPU hours; $d = 3$, $n = 32$ took 5000 CPU hours; $d = 4$, $n = 26$ took 180 CPU hours; and the arbitrary dimension calculation for $n = 24$ took a total of 980 CPU hours. The lace graph enumerations were performed on edda, a Linux cluster of Power5 CPUs at VPAC. The $d = 3$, $n = 30$ calculation took 14400 CPU hours, and the arbitrary dimensional calculation for $n = 24$ took 3400 CPU hours. Thus the total CPU time was 15000 hours for the calculation of c_{30} in $d = 3$, and 4400 hours for c_{24} for all dimensions.

1.3. Expansions in powers of $1/d$

Let $\mu = \lim_{n \to \infty} c_n^{1/n}$ denote the connective constant (a well-known subadditivity lemma gives existence of the limit [29]). It is proved in [32] that μ has an asymptotic expansion in powers of $1/d$, to all orders, with integer coefficients. Using our lace graph enumerations, we find that

$$\begin{aligned} \mu = \; & 2d - 1 - \frac{1}{2d} - \frac{3}{(2d)^2} - \frac{16}{(2d)^3} - \frac{102}{(2d)^4} - \frac{729}{(2d)^5} - \frac{5533}{(2d)^6} - \frac{42229}{(2d)^7} \\ & - \frac{288761}{(2d)^8} - \frac{1026328}{(2d)^9} + \frac{21070667}{(2d)^{10}} + \frac{780280468}{(2d)^{11}} + O\left(\frac{1}{(2d)^{12}}\right). \end{aligned} \tag{1}$$

Kesten proved that $\mu = 2d - 1 - \frac{1}{2d} + O((\frac{1}{2d})^2)$ [42]. The coefficients in (1) up to and including $102(2d)^{-5}$ were computed previously in [14, 32, 52] (with rigorous error estimate in [32]). The other seven coefficients in (1) are new, and the error estimate is rigorous. The above expansion would appear to have radius of convergence zero, but we have no proof of this. The critical temperature of the spherical model is known to have an asymptotic $1/d$ expansion with radius of convergence zero [19], and the suggestion that this is true rather generally for $1/d$ expansions of critical points was made in [15]. Note the change in sign at the term $(2d)^{-10}$; a similar sign change is observed in [19] for the critical temperature of the spherical model. An interesting mathematical question is to what degree the exact value of μ could be recovered from knowledge of all the coefficients in its $1/d$ expansion, but we do not attempt to answer that question here.

For dimensions $d \geq 5$, the lace expansion is used in [31] to prove that there is an $\epsilon > 0$ such that c_n and the mean-square displacement obey the asymptotic formulas

$$c_n = A\mu^n[1 + O(n^{-\epsilon})], \qquad \bar{\rho}_n = Dn[1 + O(n^{-\epsilon})], \tag{2}$$

with $1 \leq A \leq 1.493$ and $1.098 \leq D \leq 1.803$ when $d = 5$. We show that A and D have the asymptotic expansions

$$\begin{aligned} A = \; & 1 + \frac{1}{2d} + \frac{4}{(2d)^2} + \frac{23}{(2d)^3} + \frac{178}{(2d)^4} + \frac{1591}{(2d)^5} + \frac{15647}{(2d)^6} + \frac{164766}{(2d)^7} + \frac{1825071}{(2d)^8} \\ & + \frac{20875838}{(2d)^9} + \frac{240634600}{(2d)^{10}} + \frac{2684759873}{(2d)^{11}} + \frac{26450261391}{(2d)^{12}} + O\left(\frac{1}{(2d)^{13}}\right), \end{aligned} \tag{3}$$

$$\begin{aligned} D = \; & 1 + \frac{2}{2d} + \frac{8}{(2d)^2} + \frac{42}{(2d)^3} + \frac{284}{(2d)^4} + \frac{2296}{(2d)^5} + \frac{21024}{(2d)^6} + \frac{210306}{(2d)^7} + \frac{2242084}{(2d)^8} \\ & + \frac{24909542}{(2d)^9} + \frac{280764914}{(2d)^{10}} + \frac{3079111998}{(2d)^{11}} + \frac{29964810674}{(2d)^{12}} + O\left(\frac{1}{(2d)^{13}}\right). \end{aligned} \tag{4}$$

This extends the series up to and including order $(2d)^{-5}$ that were reported in [17, 52] and [51] for A and D, respectively (the expansion to order $(2d)^{-2}$ was obtained in [32]), and also provides rigorous error estimates.

1.4. Series analysis

We have performed extensive analysis of several series in dimensions $3 \leq d \leq 8$, using the method of differential approximants, the ratio method of Zinn-Justin, and direct fits [26]. In each dimension, we estimate the connective constant μ. For $d = 3$, we also estimate the critical amplitudes A, D and exponents γ, ν in the asymptotic formulas $c_n \sim A\mu^n n^{\gamma-1}$, $\bar{\rho}_n \sim Dn^{2\nu}$ (for which there is overwhelming evidence but no rigorous proof), as well as the exponent α in the formula $p_n \sim B\mu^n n^{\alpha-3}$. For $d = 4$, there is overwhelming evidence but no proof that $c_n \sim A\mu^n(\log n)^{1/4}$ and $\bar{\rho}_n \sim Dn(\log n)^{1/4}$ (for rigorous results on a 4-dimensional *hierarchical* lattice, see [3]); we are only able to obtain imprecise estimates for the amplitudes A, D. For $d \geq 5$, we estimate the amplitudes A, D in Eqn. (2). The results of our series analysis are tabulated and compared with other approaches in Section 7.

1.5. Outline of paper

The rest of the paper is organized as follows. In Section 2, we describe a new method of enumerating self-avoiding walks and polygons using an algorithmic improvement that we call the *two-step method*. In Section 3, we derive the lace expansion and show how it can be used to reduce the enumeration of c_n and ρ_n to the enumeration of self-avoiding polygons and other lace graphs. In addition, in Section 3.3, we show that the enumeration of c_n and ρ_n for $n \leq 24$ in dimensions $d \leq 12$ is sufficient to obtain the enumerations for $n \leq 24$ in *all* dimensions. In Section 4, we discuss the $1/d$-expansion for the connective constant μ and the critical amplitudes A and D, and show how our enumerations lead to the expansions reported above. In Section 5, we review the methods of series analysis that we implement in Section 6 to obtain the conclusions reported in Section 7. The Appendix contains tables of enumerations.

2. Enumeration methodology: the two-step method

We begin in Section 2.1 with a brief discussion of enumeration of SAWs using a backtracking algorithm, and then discuss enumeration of self-avoiding polygons in Section 2.2. An improvement on brute force enumeration which we call the *two-step method* decreases the exponential complexity of the problem, and is discussed in Section 2.3.

2.1. Enumeration of SAWs via brute force

The standard approach to the enumeration of SAWs using brute force enumeration via a backtracking algorithm has a history spanning over half a century (see Section 7.3 of [38] for many references). To make efficient use of symmetry, we classify SAWs according to the total number δ of dimensions they explore. The values of δ for an n-step SAW must lie between 1 and the minimum of d and $\frac{n}{2}$, i.e., $1 \leq \delta \leq (d \wedge \frac{n}{2})$. Let $c_{n,\delta}$ denote the contribution to c_n due to walks which explore a total of δ dimensions, with the first step taken in the positive 1-direction, the first step out of this line taken in the positive 2-direction, the first step taken out of this plane in the positive 3-direction, and so on. Then

$$c_n = \sum_{\delta=1}^{d \wedge \frac{m}{2}} \alpha_d(\delta) c_{n,\delta} \quad \text{with} \quad \alpha_d(\delta) = \prod_{j=0}^{\delta-1} (2d - 2j). \tag{5}$$

This results in a reduction in the number of distinct SAW configurations by a factor $\alpha_d(\delta)$ for a configuration occupying δ out of d possible dimensions, e.g., $\alpha_2(2) = 4 \times 2 = 8$ and $\alpha_3(3) = 6 \times 4 \times 2 = 48$.

The backtracking algorithm works recursively by generating all k step self-avoiding walks, and then appending an extra step in all possible ways, until n steps have been added. The complexity of the algorithm is given by the number of nodes of the search tree, which in our case is the sum of the number of self-avoiding walks c_k with $k \leq n$, i.e. the time τ for the algorithm to enumerate all self-avoiding walks up to length n is

$$\tau(n) \sim c_1 + c_2 + c_3 + \cdots + c_n \sim \mu^n$$

where constant and power law factors have been dropped. Thus the complexity of the algorithm is μ. There have been some improvements on the basic method, notably dimerization and trimerization [28, 46, 61], and although these improvements have allowed existing series for self-avoiding walks to be extended, none has changed the complexity of the algorithm. Our new approach, the two-step method described in Section 2.3 below, does reduce the complexity.

The self-avoidance constraint is maintained by checking whether the neighbors of the tail of the walk have previously been visited. In low dimensions (in practice for $d \leq 4$ for our implementation) it is possible to use an array to keep track of the state of all sites in the lattice. For higher dimensions the lattice becomes too large to fit into memory, and so a hash table (see, e.g., [44, 49]) is used instead, where as a site is visited it is added to the hash table. Our implementation used a hash table with linear probing, and in practice was about a factor of two slower than using an array.

2.2. Enumeration of self-avoiding polygons

The first of the lace graphs, $\pi^{(1)}_{m,\delta}$, are also known as *self-avoiding returns*. A SAP is an unrooted unoriented self-avoiding return, so that the number p_m of SAPs obeys $p_m = \frac{1}{2m}\pi^{(1)}_m$. Self-avoiding returns must have an even number $2n$ of steps, n of which are in the positive coordinate directions, and n in the corresponding negative directions. We categorize self-avoiding returns by partitioning n according to the number of steps in each positive direction.

The problem of enumeration of SAPs in general dimensions was addressed in [60], where it was noted that enumeration of all SAPs with a given partition is most efficient if it is ensured that the first step is taken in the direction with the smallest number of steps. For example, if $d = 2$, $n = 3$, with partition $[1, 2]$, then by taking the first step in the $+1$ direction we will enumerate half the number of self-avoiding returns compared to taking the first step in the $+2$ direction. A slight improvement on this idea was used in this work, where instead of choosing the first step in the direction with the smallest number of steps, the first direction is chosen as that with the smallest sum of equal values in the partition. For example, for the partition $[3, 2, 2]$, if the first step is in the $+1$ direction then we will count 3 times the number of SAPs with this partition, whereas if we choose a first step in the (indistinguishable) $+2$ or $+3$ directions, then we will count $2 + 2 = 4$ times this number.

For small n, improvements in the efficiency of the algorithm are of the expected $O(n)$, however the major failing of this method is that for large enough n, the most numerous self-avoiding polygons are those with nearly an equi-partition of step directions. Fortunately, for our domain of interest, namely $d \geq 3$, $n \leq 32$, the partition method results in a significant increase in efficiency, particularly for $d \geq 4$.

2.3. Two-step method

Backtracking enumeration algorithms take time which is dominated by the number of leaves of the search tree. The two-step method is a modification of brute force enumeration which exponentially decreases the number of leaves in the search tree and hence results in a decrease in the complexity of the algorithm. In this section, we describe this method for the enumeration of SAWs.

A *2-step walk* Ω is a SAW which takes steps chosen from $\pm e_i \pm e_j$ where the e_k are the standard unit vectors. To each such Ω taking n steps we associate a *weight* $W(\Omega)$, which is the number of $2n$-step SAWs whose restriction to every second vertex is Ω. Then we can enumerate $2n$-step walks by summing the weights of all Ω that take n steps.

To compute the weight $W(\Omega)$ of a 2-step walk, we use the *allocation graph* illustrated in Fig. 1 and defined as follows. For a 2-step in which both steps are in the same direction, we introduce a loop rooted at the midpoint of the 2-step. For a diagonal 2-step, we introduce an edge which is a perpendicular bisector (in the same 2-dimensional plane as the 2-step itself). The result is the graph $\mathcal{G}_\Omega$ depicted in Fig. 1, which consists of connected components X (with one loop), Y (with one cycle), and Z (a tree). We partition the set of connected components of $\mathcal{G}_\Omega$ into the following four categories:

- $\mathcal{T}_\Omega$ is the set of connected components of $\mathcal{G}_\Omega$ which are trees
- $\mathcal{C}_\Omega$ is the set of connected components of $\mathcal{G}_\Omega$ which contain exactly one cycle but no loop
- $\mathcal{L}_\Omega$ is the set of connected components of $\mathcal{G}_\Omega$ which contain exactly one loop but no cycle
- $\mathcal{C}^+_\Omega$ is the set of connected components of $\mathcal{G}_\Omega$ in which the number of loops and/or cycles is at least two.

Let N_T denote the number of vertices of a tree T. Finally, we set

$$I_\Omega = \begin{cases} 1 & \text{if } \mathcal{C}^+_\Omega = \varnothing \\ 0 & \text{otherwise.} \end{cases} \tag{6}$$

Theorem 2.1. *The weight of a 2-step walk Ω is given by*

$$W(\Omega) = I_\Omega 2^{|\mathcal{C}_\Omega|} \prod_{T \in \mathcal{T}_\Omega} N_T. \tag{7}$$

Proof. A SAW consistent with Ω can be regarded as an allocation of a vertex in $\mathcal{G}_\Omega$ to each 2-step in Ω, subject to the restriction that each 2-step is allocated a distinct vertex which is a possible intermediate step for that 2-step. We represent this allocation by an arrow on each edge in $\mathcal{G}_\Omega$ pointing to the chosen vertex, i.e., by an orientation of the allocation graph. An *admissible* orientation is one with at most one arrow pointing towards each vertex, i.e., with *in-degree* at most 1 at each vertex of the oriented allocation graph. The weight $W(\Omega)$ is thus equal to the number of admissible

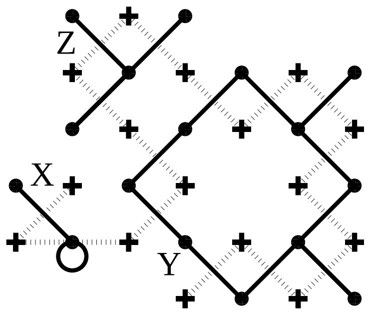

Figure 1. The allocation graph (solid lines) of a 2-step walk (broken lines), with connected components X, Y, and Z.

orientations of the allocation graph $\mathcal{G}_\Omega$. We show the admissible orientations of the various components of the allocation graph of Fig. 1 in Fig. 2.

It is plain that the number of admissible orientations of $\mathcal{G}_\Omega$ is equal to the product of the number of admissible orientations of each connected component. For each type of component, this number is as follows:

- For a tree $T \in \mathcal{T}_\Omega$, an admissible orientation is characterized by a choice of one vertex to serve as a *source*, from which all arrows point away. Thus there are N_T admissible orientations.
- For a component in $\mathcal{L}_\Omega$, removal of the single loop results in a tree, and the arrow on the loop forces the vertex on the loop to be the source for the tree. Thus there is exactly one admissible orientation.
- For a component in $\mathcal{C}_\Omega$, there are two ways to orient the cycle, and each choice allocates sources for any branches off the cycle. Thus there are exactly two admissible orientations.
- There are no admissible allocations for a component in $\mathcal{C}^+_\Omega$. This is easily verified for cycles which overlap in the form of a Θ and also for dumbbell graphs, and the general case is similar.

Together, these observations complete the proof. □

The data structure that we implement to represent an allocation graph must be able to perform several operations quickly for dynamical backtracking, such as pruning a tree, concatenation of components, identifying the size of a tree, and so on. It is straightforward to construct a data structure which allows these operations, so we do not give the details of our choice here. In our implementation, it takes $O(\log n)$ time, for a tree of n vertices, to perform the query operations, and $O(1)$ time to perform the other operations.

The extension of the two-step method to the enumeration of self-avoiding polygons is straightforward, even when combined with the partitioning of step directions as described in Section 2.2.

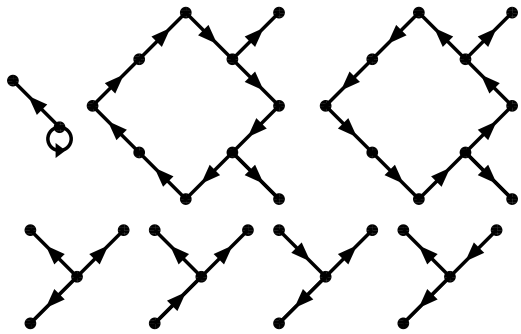

Figure 2. Admissible orientations of the connected components of the allocation graph of Fig. 1.

Complexity of the two-step and k-step methods

It is natural to ask why we are only using the two-step method, rather than the three-step, four-step, or k-step methods. Our partial answer to this question has to do with the computational complexity of the k-step methods. Suppose that we wish to enumerate all SAWs of length $n = kl$. There are two aspects to the computational complexity: the time required to enumerate all k-step walks of length l, and the time required to compute the weight of each of these k-step walks. Let us begin with the first of these issues.

The usual subadditivity argument [29] shows that the number $C_l^{(k)}$ of k-step walks of length l grows exponentially with some growth rate $\lambda = \lambda_k$. Easy upper and lower bounds on λ can be calculated in the usual way. For the upper bound, if we only disallow immediate reversals then we see that if S is the number of sites reachable by a SAW in k steps, then

$$C_l^{(k)} \leq S(S-1)^{l-1} = S(S-1)^{(n-k)/k}. \tag{8}$$

In particular, for $k = 2$, since $S = 8$ for the square lattice this gives

$$\lambda_2 \leq \sqrt{7} = 2.645\cdots, \tag{9}$$

and since $S = 18$ for the simple cubic lattice, it gives

$$\lambda_2 \leq \sqrt{17} = 4.123\cdots. \tag{10}$$

A generalization even to three-step would result in a significant improvement in this upper bound, since for the simple cubic lattice there are $S = 44$ potential end sites in three steps, and hence

$$\lambda_3 \leq \sqrt[3]{S-1} = 3.503\cdots. \tag{11}$$

Note that exponential lower bounds on $C_l^{(k)}$ can also easily be computed. For example, for $k = 2$, if we allow 2-steps only in the positive coordinate directions on the d-dimensional cubic lattice then we see that

$$C_l^{(2)} \geq \left(d + \tbinom{d}{2}\right)^l = \left(d + \tbinom{d}{2}\right)^{n/2}, \tag{12}$$

and hence

$$\lambda_2 \geq \sqrt{d + \binom{d}{2}}. \tag{13}$$

Next, we turn to the algorithmic complexity of the determination of the weight $W(\Omega)$ of a given k-step walk Ω of length l. For the case $k = 2$, the formula (7) can be computed in $O(n)$ time because the allocation graph of Ω can be calculated in $O(n)$ time, and the weight can then be calculated in $O(n)$ time using depth first search on each of the connected components to count the number of vertices (for trees), and determine if there are one or more cycles (as soon as a second cycle is detected the weight must vanish). Thus this part of the computation does not affect the exponential complexity, which remains λ_2. In practice, we find that λ_2 is roughly 2.4 for $d = 2$, and roughly 4.0 for $d = 3$. These measured values are less than $\mu \approx 2.638$ for $d = 2$ and $\mu \approx 4.68$ for $d = 3$; indeed for $d = 3$ the upper bound $\sqrt{17} = 4.123\cdots$ is already less than μ. Thus the two-step method provides an exponential improvement by reducing the complexity.

We refer to a SAW of length k that could possibly interpolate a given k-step of Ω as a *subwalk*, and we regard a subwalk as consisting of the k vertices on the subwalk omitting the initial vertex. The *subwalk graph* of Ω is the graph $\mathcal{S}_\Omega$ defined as follows. The vertex set of $\mathcal{S}_\Omega$ is the set of all possible subwalks of Ω. For SAWs we treat the origin as a special case, adding the zero-step walk consisting of the origin to the subwalk graph. A pair of subwalks forms an edge of $\mathcal{S}_\Omega$ if the two subwalks intersect each other. In particular, the subwalks which interpolate any given k-step of Ω form a clique (complete subgraph) in $\mathcal{S}_\Omega$, since they all intersect at the later endpoint of the step. Note that if there is only one subwalk we refer to a single vertex as a clique. The weight $W(\Omega)$ is the number of ways of assigning non-intersecting subwalks to each step of Ω; in other words, $W(\Omega)$ is the number of independent sets of size $l + 1$ in $\mathcal{S}_\Omega$ (every independent set must include the origin). The presence of the cliques noted above implies that no independent set contains more than $l + 1$ vertices of $\mathcal{S}_\Omega$, so when the weight $W(\Omega)$ is non-zero it corresponds to the number of maximum independent sets of the subwalk graph.

When $k = 2$ we can map the subwalk graph to an allocation graph and hence calculate the weight in $O(n)$ time. In contrast, for $k \geq 3$, the subwalk graphs can be considerably more complicated. The maximum independent set problem for general graphs is NP-complete, and we have no reason to believe that the subwalk graphs necessarily belong to a class of graphs for which the maximum independent set problem can be solved in polynomial time. If not, then the time necessary to update the weight factor is exponential in the number of vertices in the graph, and hence in the number of steps taken in the walk. Indeed it would be exponentially hard to determine if the weight factor is zero! On the other hand, it may be that for small k there exists an algorithm to enumerate independent sets that has sufficiently small complexity that the overall algorithm is still faster than the two-step method, or that there exists an algorithm that is sub-exponential or fast on average for the graphs generated by the k-step method. This line of thought merits further development, but we have not pursued it further here, and we performed our enumerations using $k = 2$.

2.4. Parallelization of the algorithm

In order to perform the enumeration of lace graphs and polygons in a reasonable amount of (calendar) time, it is necessary to divide the workload among many computers. It is possible to parallelize backtracking algorithms by truncating the backtracking tree at a fixed level, and dividing the computation beyond that level between different machines. We did this in the enumeration of polygons and lace graphs (defined in Section 3), by truncating the backtracking tree at 6 and 8 steps respectively, and saving the configurations so generated to a file. We then split the file in order to run the backtracking algorithm with distinct sets of starting configurations on multiple machines.

3. The lace expansion

In Sections 3.1–3.2, we give a quick sketch of the derivation of the lace expansion, which is the basis of our method. Further details can be found in the original paper [4], or, for a more recent account, [59]. In Sections 3.3–3.4, we discuss the enumeration of the lace graphs.

3.1. The recursion relation

Let $c_0(x) = \delta_{0,x}$, and, for $n \geq 1$, let $c_n(x)$ denote the number of n-step self-avoiding walks that begin at the origin and end at $x \in \mathbb{Z}^d$. The lace expansion gives rise to a function $\pi_m(x)$, defined below, such that for $n \geq 1$,

$$c_n(x) = \sum_{y \in \mathbb{Z}^d : |y|=1} c_{n-1}(x-y) + \sum_{m=2}^{n} \sum_{y \in \mathbb{Z}^d} \pi_m(y) c_{n-m}(x-y). \tag{14}$$

Let $D(x) = \frac{1}{2d}$ if $|x| = 1$ and otherwise $D(x) = 0$, and let $\hat{f}(k) = \sum_{x \in \mathbb{Z}^d} f(x) e^{ik \cdot x}$ (for $k = (k_1, \ldots, k_j) \in [-\pi, \pi]^d$) denote the Fourier transform of the function f. Then $\hat{D}(k) = d^{-1} \sum_{j=1}^{d} \cos k_j$. Fourier transformation of (14) gives

$$\hat{c}_n(k) = 2d\hat{D}(k)\hat{c}_{n-1}(k) + \sum_{m=2}^{n} \hat{\pi}_m(k)\hat{c}_{n-m}(k). \tag{15}$$

In particular, since $c_n = \hat{c}_n(0)$, if we write $\pi_m = \hat{\pi}_m(0)$ then (15) yields

$$c_n = 2dc_{n-1} + \sum_{m=2}^{n} \pi_m c_{n-m}. \tag{16}$$

Thus knowledge of the coefficients π_m for $2 \leq m \leq n$ allows for the recursive determination of c_n.

Let $\rho_n = \sum_x |x|^2 c_n(x)$ and $r_m = \sum_x |x|^2 \pi_m(x)$. Application of $-\sum_{i=1}^d \frac{\partial^2}{\partial k_i^2}\Big|_{k=0}$ to (15) leads to the recursion

$$\rho_n = 2dc_{n-1} + 2d\rho_{n-1} + \sum_{m=2}^{n} r_m c_{n-m} + \sum_{m=2}^{n} \pi_m \rho_{n-m}. \tag{17}$$

Thus knowledge of the coefficients c_m, π_m, r_m for $2 \le m \le n$ allows for the recursive determination of ρ_n.

3.2. *Definition of* $\pi_m(x)$

In this section, we define $\pi_m(x)$ and sketch the derivation of (14). Let $\mathcal{W}_m(x)$ denote the set of all m-step simple random walk paths (possibly self-intersecting) that start at the origin and end at x. Given $\omega \in \mathcal{W}_m(x)$, let

$$U_{st}(\omega) = \begin{cases} -1 & \text{if } \omega(s) = \omega(t) \\ 0 & \text{if } \omega(s) \neq \omega(t). \end{cases} \tag{18}$$

Then

$$c_n(x) = \sum_{\omega \in \mathcal{W}_n(x)} \prod_{0 \le s < t \le n} (1 + U_{st}(\omega)), \tag{19}$$

since the product is equal to 1 if ω is a self-avoiding walk and is equal to 0 otherwise. We call any set of pairs st, with $s < t$ chosen from $\{0, 1, 2, \ldots, n\}$, a *graph*. Let $\mathcal{B}_n$ denote the set of all graphs. Expansion of the product in (19) gives

$$c_n(x) = \sum_{\omega \in \mathcal{W}_n(x)} \sum_{\Gamma \in \mathcal{B}_n} \prod_{st \in \Gamma} U_{st}(\omega). \tag{20}$$

A graph $\Gamma \in \mathcal{B}_n$ is said to be *connected*‡ if both 0 and n are endpoints of edges in Γ, and if in addition, for any integer $c \in (0, n)$, there are $s, t \in [0, n]$ such that $s < c < t$ and $st \in \Gamma$. In other words, Γ is connected if, as intervals of real numbers, $\cup_{st \in \Gamma}(s, t)$ is equal to the connected interval $(0, n)$. The set of all connected graphs on $[0, n]$ is denoted $\mathcal{G}_n$. If we partition the sum over connected graphs according to whether: (a) 0 does not occur in an edge in the graph, or (b) 0 does occur in an edge, then we are led to the identity (14) with

$$\pi_m(x) = \sum_{\omega \in \mathcal{W}_m(x)} \sum_{\Gamma \in \mathcal{G}_m} \prod_{st \in \Gamma} U_{st}(\omega). \tag{21}$$

Case (a) gives rise to the first term on the right-hand side of (14), and case (b) gives rise to the second term, with $[0, m]$ the extent of the connected component containing 0.

An important alternate representation for $\pi_m(x)$ can be obtained in terms of laces. A *lace* is a minimally connected graph, i.e., a connected graph for which the removal of any edge would result in a disconnected graph. The set of laces on $[0, m]$ is denoted by

‡ This is not the standard graph-theory definition of a connected graph.

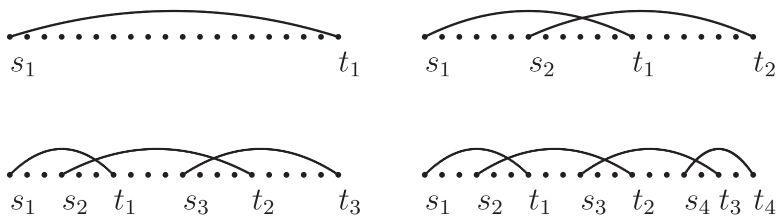

Figure 3. Laces in $\mathcal{L}_m^{(N)}$ for $N = 1, 2, 3, 4$, with $s_1 = 0$ and $t_N = m$.

$\mathcal{L}_m$, and the set of laces in $\mathcal{L}_m$ which consist of exactly N edges is denoted $\mathcal{L}_m^{(N)}$. See Fig. 3.

Given a connected graph $\Gamma \in \mathcal{B}_m$, the following prescription associates to Γ a unique lace $\mathsf{L}_\Gamma \subset \Gamma$: The lace L_Γ consists of edges $s_1t_1, s_2t_2, \ldots$, with $t_1, s_1, t_2, s_2, \ldots$ determined, in that order, by

$$t_1 = \max\{t : 0t \in \Gamma\}, \quad s_1 = 0,$$

$$t_{i+1} = \max\{t : \exists s < t_i \text{ such that } st \in \Gamma\}, \quad s_{i+1} = \min\{s : st_{i+1} \in \Gamma\}.$$

Given a lace L, the set of all edges $st \notin L$ such that $\mathsf{L}_{L\cup\{st\}} = L$ is denoted $\mathcal{C}(L)$. Edges in $\mathcal{C}(L)$ are said to be *compatible* with L.

We write $L \in \mathcal{L}_m^{(N)}$ as $L = \{s_1t_1, \ldots, s_Nt_N\}$, with $s_l < t_l$ for each l. The fact that L is a lace is equivalent to a certain ordering of the s_l and t_l. For $N = 1$, we simply have $0 = s_1 < t_1 = m$. For $N \geq 2$, $L \in \mathcal{L}_m^{(N)}$ if and only if

$$0 = s_1 < s_2, \quad s_{l+1} < t_l \leq s_{l+2} \quad (l = 1, \ldots, N-2), \quad s_N < t_{N-1} < t_N = m \tag{22}$$

(for $N = 2$ the vacuous middle inequalities play no role); see Fig. 3. Thus L divides $[0, m]$ into $2N - 1$ subintervals:

$$[s_1, s_2],\ [s_2, t_1],\ [t_1, s_3],\ [s_3, t_2],\ \ldots\ , [s_N, t_{N-1}],\ [t_{N-1}, t_N]. \tag{23}$$

Of these, intervals number 3, 5, ..., $(2N-3)$ can have zero length for $N \geq 3$, whereas all others have length at least 1.

The sum over connected graphs can be achieved by summing over laces L and over connected graphs for which the above prescription produces L. A resummation of the sum over connected graphs then leads to the formula

$$\pi_m(x) = \sum_{\omega \in \mathcal{W}_m(x)} \sum_{L \in \mathcal{L}_m} \prod_{st \in L} U_{st}(\omega) \prod_{s't' \in \mathcal{C}(L)} (1 + U_{s't'}(\omega)). \tag{24}$$

For details, see [4] or [59]. We restrict the sum in (24) to laces with N edges, and introduce a minus sign to obtain a non-negative integer, to define

$$\pi_m^{(N)}(x) = \sum_{\omega \in \mathcal{W}_m(x)} \sum_{L \in \mathcal{L}_m^{(N)}} \prod_{st \in L} (-U_{st}(\omega)) \prod_{s't' \in \mathcal{C}(L)} (1 + U_{s't'}(\omega)). \tag{25}$$

Figure 4. Self-intersections required for a walk ω with $\prod_{st\in L} U_{st}(\omega) \neq 0$, for the laces with $N = 1, 2, 3, 4$ bonds depicted in Fig. 3. The picture for $N = 11$ is also shown. A slashed subwalk may have length zero.

The right hand side of (25) is zero unless $N < m$ (since otherwise $\mathcal{L}_m^{(N)}$ is empty), and hence

$$\pi_m(x) = \sum_{N=1}^{m-1} (-1)^N \pi_m^{(N)}(x). \tag{26}$$

Note that each term in the sum (25) is either 0 or 1. The first product in (25) is equal to 1 precisely when $\omega(s) = \omega(t)$ for each edge $st \in L$. The second product is equal to 1 precisely when $\omega(s') \neq \omega(t')$ for each $s't' \in \mathcal{C}(L)$. Thus the edges in the lace require ω to have certain self-intersections, while the compatible edges enforce certain self-avoidance conditions. The self-intersections required are illustrated in Fig. 4. The simplest term is $\pi_m^{(1)}(x)$, which is zero if $x \neq 0$, and which is the number of m-step self-avoiding returns to the origin when $x = 0$. Thus $\pi_m^{(1)}(x)$ can be expressed in terms of the number of self-avoiding polygons by $\pi_m^{(1)}(x) = 2mp_m\delta_{x,0}$. For $N \geq 2$, $\pi_m^{(N)}(x)$ counts m-step walk configurations as indicated in Fig. 4. The number of loops in a diagram is equal to the number of edges in the corresponding lace. In these diagrams, each line represents a self-avoiding walk. The lines which are slashed correspond to subwalks which may consist of zero steps, but the others correspond to subwalks consisting of at least one step. The combined number of steps taken by all the subwalks is m. If the $2N-1$ subwalks in the N-loop diagram are sequentially labeled $1, 2, \ldots, 2N-1$, then the subwalks are mutually avoiding (apart from the required intersections) with the following patterns: [123] for $N = 2$; [1234], [345] for $N = 3$; [1234], [3456], [567] for $N = 4$; [1234], [3456], [5678], [789] for $N = 5$; and so on for larger N. In the above, e.g., for $N = 4$, the meaning is that subwalks $1, 2, 3, 4$ are mutually avoiding apart from the enforced intersections explicitly depicted, as are subwalks $3, 4, 5, 6$ and subwalks $5, 6, 7$. However, subwalks not grouped together are permitted to freely intersect, e.g., for $N = 4$, subwalks $1, 2$ are permitted to intersect subwalks $5, 6, 7$, and subwalks 3 and 4 can intersect subwalk 7.

The two-loop diagram $\pi_m^{(2)}$ is closely related to what are often called theta graphs. Differences are that $\pi_m^{(2)}(x)$ includes 'trivial' loops in which the first or last step immediately reverses its predecessor, or the last step equals the first step, and also $\pi_m^{(2)}$ involves oriented walks and is rooted at the origin. Taking these differences into account, we find that

$$\theta_n = \frac{1}{2}\frac{1}{3!}\left(\pi_n^{(2)} - 3\pi_{n-1}^{(1)}\right), \quad R_n = \frac{1}{2}\frac{1}{3!}\left(r_n^{(2)} - 3\pi_{n-1}^{(1)}\right), \tag{27}$$

where θ_n counts the number of n-step theta graphs, and R_n is the number weighted by the square of the distance between the two vertices of degree 3.

3.3. Decomposition by dimension

Let $\pi_m^{(N)} = \sum_x \pi_m^{(N)}(x)$ and $r_m^{(N)} = \sum_x |x|^2 \pi_m^{(N)}(x)$. Our basic task is to determine

$$\pi_m = \sum_{N=1}^{m-1} (-1)^N \pi_m^{(N)} \quad \text{and} \quad r_m = \sum_{N=1}^{m-1} (-1)^N r_m^{(N)}. \tag{28}$$

As in Section 2.1, to make efficient use of symmetry, we classify contributions to (25) according to the total number δ of dimensions explored by the m-step walk ω. Let $\pi_{m,\delta}^{(N)}$ denote the contribution to $\pi_m^{(N)}$ due to walks which explore a total of δ dimensions, with the first step taken in the positive 1-direction, the first step out of this line taken in the positive 2-direction, the first step taken out of this plane in the positive 3-direction, and so on. Then

$$\pi_m^{(N)} = \sum_{\delta=1}^{d \wedge \frac{m}{2}} \alpha_d(\delta) \pi_{m,\delta}^{(N)} \quad \text{with} \quad \alpha_d(\delta) = \prod_{j=0}^{\delta-1} (2d - 2j). \tag{29}$$

Similarly, let $r_{m,\delta}^{(N)}$ denote the contribution to $r_m^{(N)}$ due to walks which explore a total of δ dimensions, with the first step taken in the positive 1-direction, the first step out of this line taken in the positive 2-direction, the first step taken out of this plane in the positive 3-direction, and so on. Then

$$r_m^{(N)} = \sum_{\delta=1}^{d \wedge \frac{m}{2}} \alpha_d(\delta) r_{m,\delta}^{(N)}. \tag{30}$$

Thus we have

$$\pi_m = \sum_{\delta=1}^{d \wedge \frac{m}{2}} \alpha_d(\delta) \pi_{m,\delta}, \qquad r_m = \sum_{\delta=1}^{d \wedge \frac{m}{2}} \alpha_d(\delta) r_{m,\delta}, \tag{31}$$

with

$$\pi_{m,\delta} = \sum_{N=1}^{m-1} (-1)^N \pi_{m,\delta}^{(N)}, \qquad r_{m,\delta} = \sum_{N=1}^{m-1} (-1)^N r_{m,\delta}^{(N)}, \tag{32}$$

and it suffices to enumerate $\pi_{m,\delta}^{(N)}$ and $r_{m,\delta}^{(N)}$. In the next section, we explain how we do so.

Interestingly, enumeration of c_n for $n \leq 2k$ and $d \leq k$ actually gives the enumeration of c_n for $n \leq 2k$ in *all* dimensions. In particular, our enumerations of c_n for $n \leq 24$ and $d \leq 12$ allow for the enumeration of c_n for $n \leq 24$ in all dimensions d. (Similar reasoning applies for r_n.) The idea is simple. Given c_n for $n \leq 2k$ and $d \leq k$, we can solve (16) for π_m for $m \leq 2k$ and $d \leq k$. From this, we can determine $\pi_{m,\delta}$ for $m \leq 2k$, $\delta \leq k$. But since $\pi_{m,\delta} = 0$ whenever $\delta > \frac{m}{2}$, this determines π_m for $m \leq 2k$ in all dimensions d, via (31). From this, (16) recursively determines c_n for $n \leq 2k$ in all dimensions d.

As a final remark, we note that an extension of our enumerations to enumerate also $\pi_m^{(N)}(x)$ would have the potential to significantly simplify the proof in [30] of mean-field behavior for SAWs in dimensions $d \geq 5$.

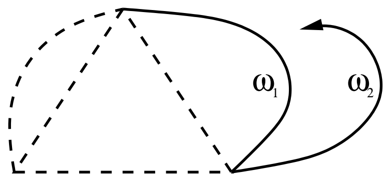

Figure 5. Generation of a lace graph via backtracking.

3.4. Enumeration of lace graphs

In this section, we describe the method used to enumerate $\pi^{(N)}_{m,\delta}$. Straightforward modifications of the method allow for the enumeration of $\rho^{(N)}_{m,\delta}$, and we do not discuss this further. Our enumerations of $\pi_{m,\delta} = \sum_{N=1}^{\infty}(-1)^N\pi^{(N)}_{m,\delta}$, p_n, c_n and r_n are given in Appendix A, and the enumerations of $\pi^{(N)}_{m,\delta}$ and $\rho^{(N)}_{m,\delta}$ on which they are based are given in [9]. We also list enumerations of θ_n and R_n (see (27)) in [9].

The case $N = 1$ amounts to the enumeration of self-avoiding polygons, which we have discussed already. For $N \geq 2$, the enumeration of lace graphs using the two-step method is significantly more complicated, due to the possibility of visiting a site multiple times, the fact that sites visited by a 2-step may belong to different subwalks, and the possibility of immediate returns. In practice, we find that the complexity of enumeration is significantly reduced from μ in the generation of 2-step lace graphs, but not to the same extent as for self-avoiding walks.

Many of the lace graphs consist of a single loop and hence contribute to $\pi^{(1)}$, and we illustrate this by calculating the ratio

$$r(m,\delta) = \frac{\pi^{(1)}_{m,\delta}}{\sum_{N=1}^{m-1}\pi^{(N)}_{m,\delta}}. \tag{33}$$

We find that $r(30,2) = 0.0625\cdots$, $r(30,3) = 0.3393\cdots$, $r(24,4) = 0.6008\cdots$, $r(24,5) = 0.7493\cdots$, and $r(24,6) = 0.8407\cdots$. For $d = 3$, $n = 30$, one can see that performing the $\pi^{(1)}$ calculation separately will reduce the running time of the algorithm by a useful amount of 34 percent. For the arbitrary dimension calculation with $m = 24$ we sum over all dimensions before calculating the ratio

$$\frac{\sum_{\delta=1}^{12}\pi^{(1)}_{24,\delta}}{\sum_{\delta=1}^{12}\sum_{N=1}^{23}\pi^{(N)}_{24,\delta}} = 0.8718\cdots, \tag{34}$$

and it indicates that 87 percent of the graphs generated for $m = 24$ are single loop graphs. Thus the enumeration of polygons is a substantial part of our analysis, and this part is performed separately.

As described in Section 3.2, the lace graphs have an interpretation in terms of a pattern of mutual avoidance between the $2N-1$ self-avoiding subwalks in an N loop graph. For enumeration purposes, these conditions are surprisingly simple, and the basic idea is as follows. In the following description (see Fig. 5):

ω_1 is a subwalk on which a loop may be completed

ω_2 is the current subwalk, which must be avoided, and
the tail of the walk is the last visited site.

First a self-avoiding return is formed, and the count for $\pi^{(1)}$ is incremented. Then ω_1 is set as the loop, and ω_2 is set as the origin. Steps are added to the graph, namely to subwalk ω_2, such that ω_2 remains self-avoiding. When contact is made with ω_1 a loop is formed and hence this configuration contributes to $\pi^{(2)}$, and then the current ω_1 is erased, and ω_1 is set to the old ω_2, while ω_2 is just set as the tail of the walk. This procedure is then repeated, as shown schematically in Fig. 5, where the part of the walk with a dashed line has been erased. Steps are added in a self-avoiding way to ω_2 until the tail reaches a site on ω_1, at which point the count for $\pi^{(N)}$ is updated, ω_1 is erased and the process starts again.

We initialize the system as follows:

$N \Leftarrow 0$ {N is the number of loops}
$m \Leftarrow 0$ {m is the length}
$\delta \Leftarrow 0$
All $\pi^{(N)}_{m,\delta}$ set to 0
Set walk ω_1 to be the origin
Set walk ω_2 to be empty
Set the origin to be occupied
tail $\Leftarrow$ origin

The procedure is described more precisely by the following pseudocode:

Recursive procedure, **Enumerate_lace**:
for all $s \in$ neighborhood(tail) **do**
  $m \Leftarrow m+1$
  if step explores a new dimension **then**
    $\delta \Leftarrow \delta+1$
  end if
  if s is empty **then**
    $\omega_2 \Leftarrow \omega_2 : s$ {append s to ω_2}
    Set s to be occupied
    tail $\Leftarrow s$
    Call **Enumerate_lace**
  else if $s \in \omega_1$ **then**
    $N \Leftarrow N+1$ {a loop has been completed}
    $\pi^{(N)}_{m,\delta} \Leftarrow \pi^{(N)}_{m,\delta} + 1$ {increment count}
    $\omega_1 \Leftarrow \omega_2$
    $\omega_2 \Leftarrow s$
    tail $\Leftarrow s$
    Call **Enumerate_lace**
  else if $s \in \omega_2$ **then**
    Do nothing {reject this step}

end if
Restore configuration
end for
Return

The exponential complexity of the algorithm will not change depending on the implementation, but it is possible to make gains in the power of n which is a factor, so we make efforts to obtain an efficient implementation. Some general considerations given on backtracking algorithms in the context of search and existence algorithms in [50] apply also for enumeration applications. For algorithms with exponential complexity, the operations which dominate the running time of the algorithm are near the leaves of the tree. This observation leads to two main conclusions regarding the design of backtracking algorithms: (a) If an expensive operation near the root of the tree can limit the number of leaves of the tree, then it will reduce the run time of the algorithm (i.e., prune near the root), and (b) Near the leaves of the tree it is important to have the basic operations run as rapidly as possible.

Our implementation used doubly linked lists for the subwalks ω_1 and ω_2, and satisfied (a) by terminating the backtracking tree whenever it could be determined that it is impossible due to geometric constraints to generate a valid lace graph from the current configuration. We implemented a fast heuristic operation to do this which takes time that is linear in the number of sites that are potential endpoints of a lace graph generated from the current configuration. In order to satisfy (b) we optimized the treatment of the final four steps by writing separate code which eliminated any expensive operations on the linked list structures.

One further technical point is that there is a bijection between lace graphs of $m+1$ steps which return immediately to the origin with their second step, and lace graphs of m steps. In our implementation, we forbade this initial immediate return, and it was a simple process to extract the correct $\pi_{m,\delta}^{(N)}$ from the resulting enumerations.

4. Expansions in powers of $1/d$

In this section, we explain how to combine our enumerations with estimates on the lace expansion to derive the $1/d$ expansions (1), (3) and (4) for the connective constant μ and for the amplitudes A and D. Let $z_c = 1/\mu$ denote the radius of convergence of the susceptibility $\chi(z) = \sum_{n=0}^{\infty} c_n z^n$. We will rely on the standard lace expansion estimate that for each $N \geq 1$ there is a constant C_N, independent of sufficiently large d, such that

$$\sum_{m=2}^{\infty}\sum_{M=N}^{\infty} m\pi_m^{(M)} z_c^m \leq C_N d^{-N}, \qquad \sum_{m=2}^{\infty}\sum_{M=N}^{\infty} r_m^{(M)} z_c^m \leq C_N d^{-N}. \tag{35}$$

The bounds (35) can be gleaned, e.g., from Section 5.4 and the solution to Exercise 5.17 of [59] ([30] has related bounds valid for all $d \geq 5$). We will supplement (35) by proving that for each $j \geq 2$, $N \geq 1$, there is a constant $C_{N,j}$, independent of large d, such that

$$\sum_{m=j}^{\infty} m\pi_m^{(N)} z_c^m \leq C_{N,j} d^{-j/2}, \qquad \sum_{m=j}^{\infty} r_m^{(N)} z_c^m \leq C_{N,j} d^{-j/2}. \tag{36}$$

4.1. $1/d$ expansion for the connective constant

It is proved in [31] that, for $d \geq 5$, z_c obeys the equation

$$z_c = \frac{1}{2d}\left[1 - \sum_{m=2}^{\infty} \pi_m z_c^m\right]. \tag{37}$$

It then follows from the first estimates of (35) and (36) that

$$z_c = \frac{1}{2d}\left[1 - \sum_{m=2}^{2N}\sum_{M=1}^{N} (-1)^M \pi_m^{(M)} z_c^m\right] + O(d^{-N-2}), \tag{38}$$

where we have used the fact proved in [32] that z_c has an asymptotic expansion in powers of d^{-1}, to replace an error term of order $d^{-N-3/2}$ by one of order d^{-N-2}. Knowledge of the coefficients $\pi_m^{(M)}$ for $m \leq 2N$ and $M \leq N$ permits the recursive calculation of the terms in the $1/d$ expansion for z_c up to and including order d^{-N-1}. Our enumerations with $m \leq 24$, $M \leq 12$ give

$$\begin{aligned} z_c = {} & \frac{1}{2d} + \frac{1}{(2d)^2} + \frac{2}{(2d)^3} + \frac{6}{(2d)^4} + \frac{27}{(2d)^5} + \frac{157}{(2d)^6} + \frac{1065}{(2d)^7} + \frac{7865}{(2d)^8} + \frac{59665}{(2d)^9} \\ & + \frac{422421}{(2d)^{10}} + \frac{1991163}{(2d)^{11}} - \frac{16122550}{(2d)^{12}} - \frac{805887918}{(2d)^{13}} + O\left(\frac{1}{(2d)^{14}}\right). \end{aligned} \tag{39}$$

Taking the reciprocal gives the $1/d$ expansion for μ stated in (1).

4.2. $1/d$ expansion for the amplitudes A and D

It is proved in [31] that for $d \geq 5$ the amplitudes A and D of (2) are given by the formulas

$$\frac{1}{A} = 2dz_c + \sum_{m=2}^{\infty} m\pi_m z_c^m, \qquad D = A\left[2dz_c + \sum_{m=2}^{\infty} r_m z_c^m\right]. \tag{40}$$

It then follows from (35) and (36) that

$$\frac{1}{A} = 2dz_c + \sum_{m=2}^{2N}\sum_{M=1}^{N} (-1)^M m\pi_m^{(M)} z_c^m + O(d^{-N-1}) \tag{41}$$

and

$$D = A\left[2dz_c + \sum_{m=2}^{2N}\sum_{M=1}^{N} (-1)^M r_m^{(M)} z_c^m\right] + O(d^{-N-1}). \tag{42}$$

Note that there can again be no fractional powers in the error estimates — it can be argued from the fact that z_c has an asymptotic expansion to all orders in powers of d^{-1}, together with the representations of $\pi_m^{(M)}$ and $r_n^{(M)}$ as polynomials in d in (31), that A

and D also have asymptotic expansions to all orders in powers of d^{-1}. Insertion of (39) and our enumerations for $m \le 24$, $M \le 12$ into (41) and (42) gives the series (3) and (4).

4.3. Proof of the error estimates (36)

It remains to prove (36). We do so in the rest of this section, by making use of notation and results from Chapters 4 and 5 of [59], and of Chapter 6 of [48] (see [35] for related ideas applied to percolation). We assume throughout this section that d is large, and we write c for a constant, possibly depending on N and j but independent of d, whose value is unimportant and may change from line to line.

Preliminaries

We will need the norms $\|f\|_\infty = \sup_{x\in\mathbb{Z}^d}|f(x)|$ and $\|f\|_2 = [\sum_{x\in\mathbb{Z}^d}|f(x)|^2]^{1/2}$ for functions $f : \mathbb{Z}^d \to \mathbb{R}$, and also the norms $\|\hat{f}\|_p = [(2\pi)^{-d}\int_{[-\pi,\pi]^d}|\hat{f}(k)|^p dk]^{1/p}$ for the Fourier transform $\hat{f}(k) = \sum_{x\in\mathbb{Z}^d} f(x)e^{ik\cdot x}$. The inverse Fourier transform is given by $f(x) = (2\pi)^{-d}\int_{[-\pi,\pi]^d}\hat{f}(k)e^{-ik\cdot x}dk$, from which we conclude that $\|f\|_\infty \le \|\hat{f}\|_1$. The Parseval relation asserts that $\|f\|_2 = \|\hat{f}\|_2$. The convolution $(f*g)(x) = \sum_y f(y-x)g(y)$ obeys $\|f*g\|_\infty \le \|f\|_2\|g\|_2$, by the Cauchy–Schwarz inequality, and $\widehat{f*g} = \hat{f}\hat{g}$.

Let $D : \mathbb{Z}^d \to \mathbb{R}$ be the one-step transition probability for simple random walk, i.e., $D(x) = \frac{1}{2d}$ if $|x| = 1$ and otherwise $D(x) = 0$. Let D^{*l} denote the convolution of l factors of D, so that $D^{*l}(x)$ is the probability that simple random walk goes from 0 to x in l steps. It is an elementary fact that the probability that a simple random walk on $\mathbb{Z}^d$ returns to its starting point after $2i$ steps obeys

$$D^{*(2i)}(0) = \int_{[-\pi,\pi]^d}\hat{D}(k)^{2i}\frac{dk}{(2\pi)^d} = \|\hat{D}^i\|_2^2 \le c_i d^{-i} \tag{43}$$

with c_i independent of the dimension d (see (3.12) of [35] for a simple proof). By the Cauchy–Schwarz inequality and the Parseval relation, it follows that

$$\|D^{*j}\|_\infty \le \|D^{*(j-1)}\|_2\|D\|_2 = \|\hat{D}^{j-1}\|_2\|\hat{D}\|_2 \le cd^{-j/2}, \tag{44}$$

and it is this inequality that will give us the desired factor $d^{-j/2}$ in (36). Direct calculation gives $\hat{D}(k) = \frac{1}{d}\sum_{j=1}^d \cos k_j$ for $k = (k_1, \ldots, k_d)$, and hence

$$\partial_j\hat{D}(k) = -\frac{1}{d}\sin k_j, \quad \partial_j^2\hat{D}(k) = -\frac{1}{d}\cos k_j, \tag{45}$$

where ∂_j denotes differentiation with respect to k_j.

Let $G_{z_c}(x) = \sum_{m=0}^\infty c_m(x)z_c^m$. It is shown in Corollary 6.2.6 of [48] that $\|G_{z_c}\|_2$ is bounded by a d-independent constant. In addition, $\|G_{z_c}*G_{z_c}\|_2 = \|\hat{G}_{z_c}\|_4^2$, and $\|\hat{G}_{z_c}\|_p$ is bounded by a d-independent constant, for any fixed p, if d is sufficiently large (depending on p). This can be shown using the infrared bound $\hat{G}_{z_c}(k) \le [1-\hat{D}(k)]^{-1}$ given in (6.2.19) of [48] or (5.36) of [59] (see Exercise 5.18(a) of [59] for the d-independence of the upper bound).

Proof of (36)

With the above preliminaries, we are now in a position to prove (36). We fix j and N and consider the sums $\sum_{m=j}^{\infty} m\pi_m^{(N)} z_c^m$ and $\sum_{m=j}^{\infty} r_m^{(N)} z_c^m$. Each is bounded using the N-loop diagram which has $2N-1$ subwalks and which consists of at least j steps. The first j steps must be allocated among a certain number of the subwalks, and we denote this number by ℓ, so that the ℓth subwalk contains the $(j+1)$st vertex (if the $(j+1)$st vertex is the last vertex of some subwalk then we take this to be the ℓth subwalk; the first vertex is the origin). We denote the length of the first $\ell-1$ subwalks by j_i for $i=1,\ldots,\ell-1$, and we set $j_\ell = j - \sum_{i=1}^{\ell-1} j_i$. The number of possibilities for ℓ and $j_1,\ldots,j_\ell$ depends only on j and N. It therefore suffices to obtain an upper bound of the form $C_{N,j}d^{-j/2}$ for the case of fixed ℓ and $j_1,\ldots,j_\ell$, and we will prove such a bound.

For the two sums of interest, namely $\sum_{m=j}^{\infty} m\pi_m^{(N)} z_c^m$ and $\sum_{m=j}^{\infty}\sum_x |x|^2\pi_m^{(N)}(x) z_c^m$, we decompose the factors m and $|x|^2$ among the subwalks using $m=\sum_{k=1}^{2N-1} m_k$ and $|x|^2 \le (2N-1)\sum_{k=1}^{2N-1}|x_k|^2$, where m_k and x_k denote the length and displacement of the kth subwalk. In either case, it suffices to estimate a single term in this decomposition, which leads us to consider an N-loop diagram in which the $(j+1)$st vertex lies in the ℓth subwalk, and in which the kth subwalk carries either a factor m_k or $|x_k|^2$. A small extension of (4.40)–(4.41) of [59] yields an upper bound

$$\|f_k\|_\infty \prod \|f_i * f_{i'}\|_\infty \tag{46}$$

where f_a is the generating function appropriate for the ath subwalk, and where the factors in the product are formed from consecutive pairs (i,i') from the set $\{1,\ldots,2N-1\}$ with k removed. We consider the three cases (i) $k>\ell$, (ii) $k<\ell$, (iii) $k=\ell$, and show that each case obeys the desired upper bound.

Case (i) $k>\ell$. In this case the factor $\|f_k\|_\infty$ is either $\sup_x \sum_{m=1}^{\infty} mc_m(x)z_c^m$ or $\sup_x |x|^2\sum_{m=1}^{\infty} c_m(x)z_c^m$. These are both bounded by a d-independent constant for large d, using Corollary 6.2.6 and (6.2.39) of [48].

The factors $\|f_i * f_{i'}\|_\infty$ with $i>\ell$ are all bounded above by $\|G_{z_c} * G_{z_c}\|_\infty \le \|G_{z_c}\|_2^2$, which is bounded by a d-independent constant as noted previously.

For the remaining factors $\|f_i * f_{i'}\|_\infty$, consider first the case $i'<\ell$. In this case we bound the generating functions above by their simple random walk counterparts to see that

$$\|f_i * f_{i'}\|_\infty \le (2dz_c)^{j_i+j_{i'}}\|D^{*(j_i+j_{i'})}\|_\infty \le cd^{-(j_i+j_{i'})/2}, \tag{47}$$

where we have used (44) and the fact that $2dz_c \le 2$ due to the elementary bound $z_c^{-1}=\mu\ge d$.

Thus it suffices to consider the cases $i=\ell$ and $i'=\ell$ and to show that in either case

$$\|f_i * f_{i'}\|_\infty \le cd^{-[j-\sum_{n'<\ell}(j_n+j_{n'})]/2}. \tag{48}$$

We show this when $i = \ell$; the case $i' = \ell$ is similar. Note that when $i = \ell$, $j - \sum_{i'<\ell}(j_i + j_{i'})$ is simply j_ℓ. When $i = \ell$ we can bound the first j_ℓ steps of the ℓth subwalk by simple random walk to obtain

$$\|f_i * f_{i'}\|_\infty \leq \|(2dz_c)^{j_\ell} D^{*j_\ell} * G_{z_c} * G_{z_c}\|_\infty. \tag{49}$$

The factor $(2dz_c)^{j_\ell}$ plays no role, and the Cauchy–Schwarz inequality gives

$$\|D^{*j_\ell} * G_{z_c} * G_{z_c}\|_\infty \leq \|D^{*j_\ell}\|_2 \|G_{z_c} * G_{z_c}\|_2 \leq cd^{-j_\ell/2}, \tag{50}$$

where we used (43) and the fact noted above that $\|G_{z_c} * G_{z_c}\|_2 \leq c$. This completes the proof in Case (i).

Case (ii) $k < \ell$. We again bound the first j steps by simple random walk. The factor $\|f_k\|_\infty$ pertains to a walk of length j_k and carries a factor $m_k = j_k$ or $|x_k|^2 \leq j_k^2$ (since the displacement cannot exceed the number of steps). These additional factors have an upper bound depending only on j and N and can thus be ignored. This factor is then bounded by $cd^{-j_k/2}$ and the rest of the argument follows as in Case (i); we omit further details.

Case (iii) $k = \ell$. In this case the factors $\|f_i * f_{i'}\|_\infty$ with $i' < \ell$ are bounded via simple random walk, as in Case (i), to give a combined upper bound $cd^{-\sum_{n<\ell} j_n/2}$. Also, the factors with $i > \ell$ are bounded above by a constant, again as in Case (i). It suffices to show that $\|f_\ell\|_\infty \leq cd^{-j_\ell/2}$.

The generating function f_ℓ has two features that we must take into account: the walks involved take at least j_ℓ steps, and there is a factor m_ℓ or $|x_\ell|^2$ present. When m_ℓ is present, we write it as $m_\ell = j_\ell + (m_\ell - j_\ell)$. When $|x_\ell|^2$ is present, we write $x_\ell = y_1 + y_2$ where y_1 is the displacement of the first j_ℓ steps and y_2 is the displacement of the remaining $m_\ell - j_\ell$ steps, and use the inequality $|x_\ell|^2 \leq 2(|y_1|^2 + |y_2|^2)$. The factors j_ℓ or $|y_1|^2$ are bounded by a constant depending only on j and N, and they can be ignored. The contribution to $\|f_k\|_\infty$ due to either of these cases is then bounded above by $\|(2dz_c)^{j_\ell} D^{*j_\ell} * G_{z_c}\|_\infty$, which is bounded above by $cd^{-j_\ell/2}$ as required, using the Cauchy–Schwarz inequality and bounds already discussed. It remains to estimate the contribution due to either $m_\ell - j_\ell$ or $|y_2|^2$.

The case of $m_\ell - j_\ell$ is easily bounded above by $\|(2dz_c)^{j_\ell} D^{*j_\ell} * G_{z_c} * G_{z_c}\|_\infty$, which as we have seen in Case (i) is at most $cd^{-j_\ell/2}$, as required. Let $X(x) = |x|^2 G_{z_c}(x)$. The remaining case, with $|y_2|^2$, contributes at most

$$\|(2dz_c)^{j_\ell} D^{*j_\ell} * X\|_\infty \leq c\|D^{*j_\ell}\|_2 \|X\|_2 = c\|\hat{D}^{j_\ell}\|_2 \|\hat{X}\|_2 \leq cd^{-j_\ell/2} \|\hat{X}\|_2. \tag{51}$$

It now suffices to show that $\|\hat{X}\|_2$ is bounded by a d-independent constant. But $\hat{X} = -\sum_{i=j}^d \partial_j^2 \hat{G}_{z_c}$, and, writing $F = 1/\hat{G}_{z_c}$ and $\Pi(x) = \sum_{m=2}^\infty \pi_m(x) z_c^m$, (6.2.24) of [48] gives

$$|\partial_j^2 \hat{G}_{z_c}| \leq c \left(\frac{|\partial_j^2 \hat{D}|}{F^2} + \frac{|\partial_j^2 \hat{\Pi}|}{F^2} + \frac{|\partial_j \hat{D}|^2}{F^3} + \frac{|\partial_j \hat{D}|\,|\partial_j \hat{\Pi}|}{F^3} + \frac{|\partial_j \hat{\Pi}|^2}{F^3} \right). \tag{52}$$

It suffices to obtain an $O(d^{-1})$ upper bound on the L^2 norm of each term on the right-hand side.

By (45), the L^2 norm of the first term on the right-hand side of (52) is at most $cd^{-1}\|\hat{G}^2_{z_c}\|_2$, which we have seen is $O(d^{-1})$. It is shown in Corollary 6.2.7 of [48] that $\partial^a_j \hat{\Pi} = O(d^{-2})$ for $a = 1, 2$. Together with our previous observation that $\|\hat{G}_{z_c}\|_6 \le c$, this is sufficient for our needs and completes the proof of the error estimates (36).

5. Analysis of series: methodology

The presumed asymptotic forms for c_n, ρ_n and p_n for $d = 3$ are given by

$$\begin{aligned} c_n \sim \mu^n n^{\gamma-1} &\left(A + \frac{a_1}{n^\theta} + \frac{a_2}{n} + \frac{a_3}{n^{1+\theta}} + \frac{a_4}{n^2} + \cdots\right) \\ &+ \mu^n (-1)^n n^{\alpha-2} \left(b_0 + \frac{b_1}{n^\theta} + \frac{b_2}{n} + \frac{b_3}{n^{1+\theta}} + \frac{b_4}{n^2} + \cdots\right), \end{aligned} \tag{53}$$

$$\begin{aligned} \rho_n \sim \mu^n n^{\gamma+2\nu-1} &\left(AD + \frac{d_1}{n^\theta} + \frac{d_2}{n} + \frac{d_3}{n^{1+\theta}} + \frac{d_4}{n^2} + \cdots\right) \\ &+ \mu^n (-1)^n n^{\alpha-2} \left(e_0 + \frac{e_1}{n^\theta} + \frac{e_2}{n} + \frac{e_3}{n^{1+\theta}} + \frac{e_4}{n^2} + \cdots\right), \end{aligned} \tag{54}$$

$$p_n \sim \mu^n n^{\alpha-3} \left(B + \frac{f_1}{n^\theta} + \frac{f_2}{n} + \frac{f_3}{n^{1+\theta}} + \frac{f_4}{n^2} + \cdots\right) \quad (n \text{ even}). \tag{55}$$

The alternating terms in the formulae for c_n and ρ_n are manifestations of a generating function singularity at $-z_c = -1/\mu$. This singularity, widely believed but not rigorously proved to exist, is known as the anti-ferromagnetic singularity due to its similarity to a corresponding singularity in the Ising model. Anti-ferromagnetic singularities are generally expected to occur on *loose-packed* (certain bipartite) lattices such as $\mathbb{Z}^d$. The fact that the polygon exponent α governs the effect of this singularity on the series has very strong numerical evidence for $d = 2$ [7, 41], and was suggested as early as [22]. As we will argue in [10], the alternating signs in the values of π_m provide direct evidence both for the existence of the anti-ferromagnetic singularity and the role of α in its behavior (see Tables 16–17 — we believe but have not proved that the alternation in sign persists for all m).

We find that the conventional assumption (see, e.g., [7, 47]) that the leading *confluent correction* θ is the same for c_n and ρ_n is well supported by our results. The series we have for p_n are too short to say anything definitive in this respect. There is an implicit assumption in the formulae above that θ is close to 0.5 and therefore integer multiples of the form $2k\theta$ are indistinguishable from integer terms, while $(2k+1)\theta \approx k+\theta$. If θ is not exactly 0.5 then this assumption must eventually break down for high-order terms in the asymptotic form.

Series analysis is a collection of methods for estimating the values of μ, γ, ν, α, etc., given the values of c_n, ρ_n, p_n for $n \le N$. For an extensive overview of methods of series analysis, see [26]. We apply the methods of differential approximants [26] (a generalization of Padé approximants, also called integral approximants [39]), the version of the ratio method due to Zinn-Justin [62, 63, 26, 5], and direct fitting of the presumed asymptotic form. In this section, we discuss each of the methods in some detail. (We have also applied Neville-Aitken extrapolation and the Brezinski θ algorithm [26], but neither of these methods produced improved results.)

5.1. *The method of differential approximants*

In the method of differential approximants, the unknown generating function is represented by the solution to an ordinary differential equation of the form:

$$\sum_{i=0}^{K} Q_i(z)\frac{d^i f}{dz^i} = P(z). \tag{56}$$

The functions P and Q_i are polynomials, of degrees L and N_i. We choose $L \leq 5$, $K = 1, 2, 3$, $N_K \geq 3$ (which guarantees at least three regular singularities), and take Q_K to have highest-order coefficient equal to 1. The order of the polynomials was chosen so that $|N_i - N_j| \leq 2$. Given coefficients $a_0, \ldots, a_N$, the polynomials P, Q_i are chosen so that the polynomial $\sum_{n=0}^{N} a_n z^n$ solves the differential equation to within an error of order z^{N+1}. This choice is made by solving a system of linear equations in $L + K + 1 + \sum_{i=0}^{K} N_i$ unknowns, determined from $N + 1$ known coefficients.

The series we analyze for $d = 3$, in particular, produce many defective approximants which have singularities near the physical singularity, or clearly incorrect singularities on or near the positive real axis, which may distort estimates of the critical point and critical exponents. We attribute this, in part, to the existence of strong confluent corrections. In practice, eliminating defective approximants does not change central estimates in the series we analyzed significantly, but does slightly reduce the spread of estimates, and especially for $K = 1, 2$ and large N, eliminates most of the approximants. This introduces a systematic bias, and it is primarily for this reason that we chose *not* to eliminate defective approximants. Instead we iteratively eliminated outliers in our analysis, for which the critical point and critical exponents differ from the mean by more than r times the standard deviation, with the subjective choice $r = 3$. We report the standard deviation of the estimates of the remaining approximants, as an indication of their spread.

It is straightforward to ensure that there is a singularity at a biased value of z_c by introducing an additional linear equation:

$$Q_K(z_c) = 0. \tag{57}$$

It is less straightforward to bias the exponent without simultaneously fixing the critical point, but this is usually achieved by plotting estimates of the exponent against z_c from unbiased estimates, and exploiting the fact that this relation is generally observed to be linear to fix the exponent and obtain a biased estimate of z_c.

For $d = 3$, as we will explain below, we find that strong confluent corrections cause the central estimates obtained from differential approximants to drift steadily, which makes it difficult to extrapolate and obtain a final value for z_c. An exception is for $\bar{\rho}_n$, for which we know that the critical value is exactly $z_c = 1$. This enables us to bias for a confluent singularity (see [26]) at $z_c = 1$ via the imposition of the linear equations:

$$Q_K(1) = Q'_K(1) = Q_{K-1}(1) = 0 \tag{58}$$

for $K \geq 2$. The confluent exponents may then be obtained as the two solutions α, β of the quadratic indicial equation

$$\frac{1}{2}(\lambda - (K-2))(\lambda - (K-1))Q''_K(1) + (\lambda - (K-2))Q'_{K-1}(1) + Q_{K-2}(1) = 0 \tag{59}$$

in λ. This equation may be written in the form

$$a\lambda^2 + b\lambda + c = 0, \tag{60}$$

and its roots obey

$$\alpha + \beta = -\frac{b}{a}, \qquad \alpha\beta = \frac{c}{a}. \tag{61}$$

The roots should be $\alpha = -2\nu - 1$ and $\beta = -2\nu - 1 + \theta$. Assume that θ is known exactly, and that we have some a priori estimate α_0 for α. Let ϵ be the error given by $\alpha = \alpha_0 + \epsilon$. Then $\beta = \alpha_0 + \theta + \epsilon = \beta_0 + \epsilon$. We substitute this into (61), drop the term of order ϵ^2 in the equation $\alpha\beta = c/a$, and then eliminate ϵ to obtain

$$a(\alpha_0^2 + \beta_0^2) + b(\alpha_0 + \beta_0) + 2c = 0. \tag{62}$$

We add this equation to those determining our differential approximant, thereby forcing the two confluent exponents to be different by θ to within $O(\epsilon^2)$. In practice this method is found to work extremely well, and is quite insensitive to the value of the biased exponent. For $d = 3$, we take α_0 to be given by $\nu = 0.5877$ or $\nu = 0.59$, and then we use the differential approximant to obtain a refined estimate of ν. Such variations in the choice of α_0 were observed to result in negligible differences in exponent estimates. For fixed ν, deviations in the observed versus the biased value of θ almost always occur in the fourth decimal place or later.

For $d \geq 5$, we have the luxury of knowing that $\nu = 1/2$, so we can bias for the dominant exponent, and the other root allows us to determine the value of θ.

5.2. *The method of Zinn-Justin*

The ratio method of Zinn-Justin [62, 63] is a nonlinear sequence extrapolation method, and may be adapted to take into account leading corrections to scaling as follows. Given a series a_n one constructs a set of unbiased estimates for the critical point and critical exponent on a loose-packed lattice via the relations

$$s_n = -\left(\log \frac{a_n a_{n-4}}{a_{n-2}^2}\right)^{-1}, \tag{63}$$

$$\bar{s}_n = \frac{1}{2}(s_n + s_{n-1}), \tag{64}$$

$$\gamma_n^u = 1 + 2\frac{\bar{s}_n + \bar{s}_{n-2}}{(\bar{s}_n - \bar{s}_{n-2})^2}, \tag{65}$$

$$\mu_n = \left(\frac{a_n a_{n-1}}{a_{n-2}a_{n-3}}\right)^{1/4} \exp\left(-\frac{\bar{s}_n + \bar{s}_{n-2}}{2\bar{s}_n(\bar{s}_n - \bar{s}_{n-2})}\right) \tag{66}$$

(reproduced from [26]). As discussed, for example, by Campostrini *et al.* [5], one then expects that the leading correction to μ_n is of order $1/n^{1+\theta}$, while for the exponent the leading correction is of order $1/n^{\theta}$. This correction can be removed by linearly extrapolating consecutive estimates to obtain a new sequence of unbiased estimates for μ and the exponent.

5.3. The method of direct fitting

The presumed asymptotic form (53) leads to the formulae:

$$\begin{aligned}\log c_n \sim n\log\mu + (\gamma-1)\log n + \log A + \frac{q_0}{n^\theta} + \frac{q_1}{n} + \frac{q_2}{n^{1+\theta}} + \cdots \\ + (-1)^n n^{\alpha-\gamma-1}\left(r_0 + \frac{r_1}{n^\theta} + \frac{r_2}{n} + \frac{r_3}{n^{1+\theta}} + \cdots\right),\end{aligned} \tag{67}$$

$$\begin{aligned}c_n/c_{n-1} \sim \mu\left(1 + \frac{\gamma-1}{n} + \frac{q_0}{n^{1+\theta}} + \frac{q_1}{n^2} + \frac{q_2}{n^{2+\theta}} + \cdots\right) \\ + \mu(-1)^n n^{\alpha-\gamma-1}\left(r_0 + \frac{r_1}{n^\theta} + \frac{r_2}{n} + \frac{r_3}{n^{1+\theta}} + \cdots\right),\end{aligned} \tag{68}$$

$$\begin{aligned}c_n/c_{n-2} \sim \mu^2\left(1 + \frac{2(\gamma-1)}{n} + \frac{q_0}{n^{1+\theta}} + \frac{q_1}{n^2} + \frac{q_2}{n^{2+\theta}} + \cdots\right) \\ + \mu^2(-1)^n n^{\alpha-\gamma-2}\left(r_0 + \frac{r_1}{n^\theta} + \frac{r_2}{n} + \frac{r_3}{n^{1+\theta}} + \cdots\right),\end{aligned} \tag{69}$$

where q_i and r_i are permitted to differ from one form to the next. Similar formulae can be derived from (54) and (55). We truncate these series at some finite order and determine the unknown quantities as the best fit to a set of linear equations.

This gives unbiased estimates of the critical point, exponent, and amplitude. It is possible to form biased estimates by fixing the value of either the growth constant or the exponent, but except when the exponent (for $d \geq 4$) or the growth constant ($\bar{\rho}_n$ series) is known exactly our preference is to use unbiased estimates to avoid the necessity of using stability as a criterion to distinguish between different biased estimates. On the other hand, we do use a biased value of $\alpha - \gamma$ in the anti-ferromagnetic term (or $\alpha - \gamma - 2\nu$ for ρ), but in practice this is unimportant for the overall fit, since the anti-ferromagnetic terms are dominated by the leading correction to scaling for the ferromagnetic part.

The asymptotic form for $\log c_n$ has the advantage that it also gives estimates for the amplitude. The ratio c_n/c_{n-1} has the disadvantage that the anti-ferromagnetic term is enhanced compared to c_n/c_{n-2}, leading to stronger odd-even oscillation. This was observed to be of little significance because the magnitude of the contribution of the anti-ferromagnetic terms to the asymptotic form remains small in comparison to the ferromagnetic terms. In practice, it was found that the c_n/c_{n-2} form produces estimates which have greater shifts as the number of terms in the fitting form are increased, for fixed n, which suggests that the coefficients in this asymptotic expansion are larger compared to those in the $\log c_n$ and c_n/c_{n-1} asymptotic expansions.

Our method is to fit the asymptotic forms using as many terms in the expansion as possible, until fits become unstable. We do this by starting with the bare minimum of terms, e.g., in the $\log c_n$ expansion we begin with $n \log \mu$, $(\gamma - 1)\log n$, and $\log A$, and successively add terms, choosing whether to add a term from the ferromagnetic or anti-ferromagnetic parts by looking at the stability of estimates. In practice, this meant alternately adding terms from the anti-ferromagnetic and ferromagnetic parts to minimize odd-even oscillations. We note that there are frequently still some residual odd-even oscillations in the fits, and as we regard this oscillation as an artifact of fitting the series with a finite number of terms, we often average adjacent estimates to obtain a smoothed sequence of estimates.

When performing the $\log c_n$ fit with the first neglected term of order $1/n^{\xi}$, we can expect that for sufficiently large n the truncation error $\epsilon(n)$ will be of the same order. Then the error in μ is of order $1/n^{\xi+1}$, the error in γ is of order $1/n^{\xi}$, and the error in the amplitude is of order $1/n^{\xi}$. If the asymptotic form is correct, one expects that a plot of μ (respectively γ, A) versus $x = 1/n^{\xi+1}$ (resp. $1/n^{\xi}$) would be linear as $x \to 0$ and approach the axis with non-zero slope. We perform the extrapolations by doing an unweighted linear least squares fit of the last 5 estimates versus the appropriate choice of $1/n^{\xi+1}$ or $1/n^{\xi}$.

We then seek to improve the extrapolations by using the technique of a fixed small 'shift' δn in n (see Section II.A of [18]). We choose δn to minimize

$$\Delta^2 = n^2 \sum_{i=0}^{4} (\mu_{n-i} - \bar{\mu})^2 + \sum_{i=0}^{4} (\gamma_{n-i} - \bar{\gamma})^2, \tag{70}$$

where μ_{n-i} is the δn-dependent estimate for μ resulting from the coefficients up to order $n - i$, and $\bar{\mu}$ is the average of $\mu_n, \ldots, \mu_{n-4}$. The details of this choice of Δ are not important, as any sensible choice will result in much the same outcome. For almost all of the cases studied there is a clear global minimum at a value of δn which is small compared to the maximum value of n, and no other local minima. This choice of δn effectively minimizes the rate of change of the estimates of μ, γ, and A. There is no guarantee that this will simultaneously minimize the error $\epsilon(n)$, but it does make it easier to extrapolate the estimates to $n \to \infty$, particularly if $d\epsilon/dn \approx 0$ in which case the final estimates become our unbiased estimates.

In Fig. 6 one can see that estimates do change as δn shifts, but only by relatively small amounts in the vicinity of the maximally stable value. As a test case, we also applied the method of direct fitting to the $\bar{\rho}_n$ series for $d = 3$ without biasing for $z_c = 1$. We find that our choice of the shift δn significantly enhances convergence of estimates of z_c to the exact value $z_c = 1$, and that the direct fitting procedure is superior by an order of magnitude as compared to the Zinn-Justin and differential approximant methods.

To gauge the accuracy of the results of the direct fits, it is clear that the spread

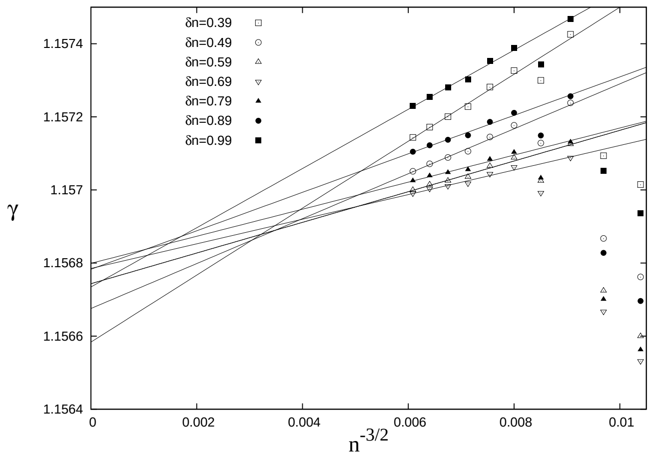

Figure 6. Estimates for γ for $d = 3$ from fit of $\log c_n$ with highest-order terms $\{q_1, r_2\}$ for different values of δn, where $\delta n = 0.69$ minimizes Δ^2.

among estimates of the same order is a lower bound on the uncertainty. If estimates from the fits are converging sufficiently rapidly as the order is increased, then the jump from the second highest-order fit to the highest-order fit *may* give some idea of the size of the uncertainty. Therefore the recipe we use to analyze series via this procedure is to find the highest-order stable fits, exclude those fits which appear to be converging anomalously slowly, and take the mean of the reliable fits as our central estimate. We then calculate the mean of the jumps from the second highest-order fits to the highest-order fits, and quote this value to give some idea of the accuracy of our central estimate. We do not claim that this is a rigorous procedure, nor that this should in any way be interpreted as a statistical error estimate.

6. Analysis of series: results

In this section, we analyze the series for c_n, ρ_n, $\bar{\rho}_n$ and p_n, using the methods discussed in Section 5. We first consider the important case $d = 3$ at length, then $d \geq 4$, and finally we analyze the $1/d$ expansion for μ. We used multiple precision floating point computations via the GMP bignum library, to ensure numerical robustness.

6.1. Analysis for $d = 3$

We first analyze the series on the cubic lattice $\mathbb{Z}^3$ for c_n, for ρ_n and $\bar{\rho}_n$, and for p_n.

6.1.1. Analysis of the series c_n

The method of differential approximants. In Table 1, we give estimates for μ and γ from second- and third-order unbiased differential approximants, where the value in parentheses is the standard deviation of the estimates after we have pruned away outliers.

Table 1. Differential approximants for c_n.

	Second-order DA			Third-order DA		
N	μ	γ	U/T	μ	γ	U/T
21	4.683846(51)	1.16198(47)	35/45	4.683831(56)	1.16213(53)	76/87
22	4.683920(43)	1.16125(47)	40/44	4.68387(11)	1.1614(11)	88/99
23	4.683921(22)	1.16119(34)	41/44	4.683904(45)	1.16131(59)	76/104
24	4.683927(16)	1.16112(25)	37/45	4.683890(38)	1.16157(39)	74/107
25	4.683931(58)	1.16092(97)	38/44	4.683937(69)	1.1606(11)	76/113
26	4.683974(33)	1.16024(78)	42/44	4.684017(41)	1.1590(12)	98/116
27	4.683999(55)	1.1594(14)	40/45	4.684017(32)	1.15907(96)	90/114
28	4.683997(34)	1.15973(94)	39/44	4.684022(13)	1.15901(47)	96/111
29	4.684038(21)	1.15842(86)	37/44	4.6840182(45)	1.15916(16)	90/114
30	4.684019(33)	1.1591(15)	44/45	4.6840224(53)	1.15900(21)	110/116

The number of approximants utilized to obtain the estimates is U, while T is the total number of approximants including the excluded outliers. The results of Table 1 reveal that the estimates for μ (γ) still have an upwards (downwards) trend as N increases. The third-order approximants suggest a value μ in the vicinity of 4.68402 and γ near 1.1590, but given that the second-order approximants have not settled down we believe this apparent convergence to be spurious, and expect that systematic shifts in μ and γ will continue.

The method of Zinn-Justin. We suppose first that $\theta = 0.5$; later we will see how estimates change under variation in θ. Application of the method of Zinn-Justin gives estimates of $\mu = 4.684024$ and $\mu = 4.684033$ for the odd and even subsequences respectively, both of which are slowly increasing with N. The exponent estimates are $\gamma = 1.15704$ and $\gamma = 1.15703$, both estimates slowly decreasing with N.

The method of direct fitting. For direct fitting, we found for each form that the highest-order fits for which smoothly changing values were observed for all coefficients have highest-order terms q_1 and r_2. We again suppose first that $\theta = 0.5$, and consider alternate possibilities for θ afterward.

Tables 2–4 show the highest-order fits for $\log c_n$, c_n/c_{n-1}, and c_n/c_{n-2}. All estimates are extremely stable, suggesting that the fitting forms of Equations (67)–(69) are basically correct. In particular, we regard the r_2 estimates in Table 3 as stable because the absolute values of successive estimates are similar and close to zero, and it is absolute rather than relative changes in value that are important, as coefficients may be genuinely close to zero.

We extrapolate the estimates from Tables 2–4, as well as the estimates from the

Table 2. Smoothed coefficients in asymptotic expansion of $\log c_n$ with $\theta = 0.5$.

N	μ	γ	A	q_0	q_1	r_0	r_1	r_2
21	4.6840569	1.15653	1.21859	-0.0693	0.0304	-0.0641	-0.0337	0.0211
22	4.6840526	1.15667	1.21773	-0.0676	0.0288	-0.0643	-0.0316	0.0166
23	4.6840343	1.15709	1.21520	-0.0628	0.0250	-0.0645	-0.0299	0.0131
24	4.6840385	1.15699	1.21577	-0.0639	0.0259	-0.0646	-0.0292	0.0113
25	4.6840356	1.15707	1.21534	-0.0630	0.0252	-0.0646	-0.0287	0.0102
26	4.6840364	1.15705	1.21545	-0.0632	0.0253	-0.0647	-0.0283	0.0094
27	4.6840371	1.15702	1.21562	-0.0636	0.0257	-0.0647	-0.0279	0.0085
28	4.6840375	1.15701	1.21566	-0.0637	0.0257	-0.0648	-0.0275	0.0075
29	4.6840376	1.15701	1.21571	-0.0638	0.0259	-0.0648	-0.0271	0.0064
30	4.6840381	1.15699	1.21579	-0.0639	0.0260	-0.0648	-0.0267	0.0053

Table 3. Smoothed coefficients in asymptotic expansion of c_n/c_{n-1} with $\theta = 0.5$.

N	μ	γ	q_0	q_1	r_0	r_1	r_2
21	4.6840409	1.15707	0.0307	-0.0279	-0.1292	-0.0559	0.0168
22	4.6840379	1.15717	0.0301	-0.0268	-0.1295	-0.0527	0.0101
23	4.6840230	1.15751	0.0281	-0.0237	-0.1298	-0.0503	0.0049
24	4.6840280	1.15739	0.0288	-0.0248	-0.1299	-0.0495	0.0030
25	4.6840272	1.15741	0.0287	-0.0247	-0.1300	-0.0491	0.0023
26	4.6840287	1.15737	0.0290	-0.0251	-0.1300	-0.0490	0.0020
27	4.6840308	1.15731	0.0294	-0.0258	-0.1300	-0.0488	0.0014
28	4.6840316	1.15728	0.0295	-0.0261	-0.1300	-0.0484	0.0005
29	4.6840326	1.15725	0.0298	-0.0266	-0.1301	-0.0480	-0.0006
30	4.6840335	1.15722	0.0299	-0.0269	-0.1301	-0.0475	-0.0017

lower-order fits. This information is summarized in Table 5, and shown graphically for the highest-order fits in Figures 7–9. The most important features of Table 5 are that the estimates for the $\log c_n$ and c_n/c_{n-1} fits seem to be converging quite rapidly, as the jumps from the $\{q_0, r_1\}$ to the $\{q_1, r_2\}$ fits appear quite small. The final jumps for the c_n/c_{n-2} fit are somewhat larger, which suggests that the coefficients in the asymptotic expansion for c_n/c_{n-2} are perhaps larger; if the coefficients are uniformly larger than those for the other fits then we would expect the c_n/c_{n-2} estimates to be less accurate.

We exclude the c_n/c_{n-2} fits, and follow the procedure of Section 5.3 to obtain the estimates in Table 13 for μ, γ, and A.

We can also obtain a range of estimates for γ by exploiting the approximately linear

Table 4. Smoothed coefficients in asymptotic expansion of c_n/c_{n-2} with $\theta = 0.5$.

N	μ	γ	q_0	q_1	r_0	r_1	r_2
21	4.6839688	1.15906	0.0352	-0.0178	0.2541	0.0826	-0.0150
22	4.6840099	1.15816	0.0450	-0.0330	0.2427	0.1768	-0.2080
23	4.6840051	1.15827	0.0436	-0.0308	0.2447	0.1587	-0.1687
24	4.6840037	1.15830	0.0433	-0.0303	0.2482	0.1282	-0.1018
25	4.6840086	1.15818	0.0449	-0.0329	0.2493	0.1183	-0.0799
26	4.6840114	1.15810	0.0458	-0.0345	0.2497	0.1145	-0.0709
27	4.6840151	1.15799	0.0472	-0.0370	0.2495	0.1168	-0.0768
28	4.6840183	1.15790	0.0484	-0.0392	0.2491	0.1205	-0.0853
29	4.6840206	1.15782	0.0494	-0.0410	0.2490	0.1216	-0.0883
30	4.6840228	1.15775	0.0503	-0.0428	0.2489	0.1225	-0.0903

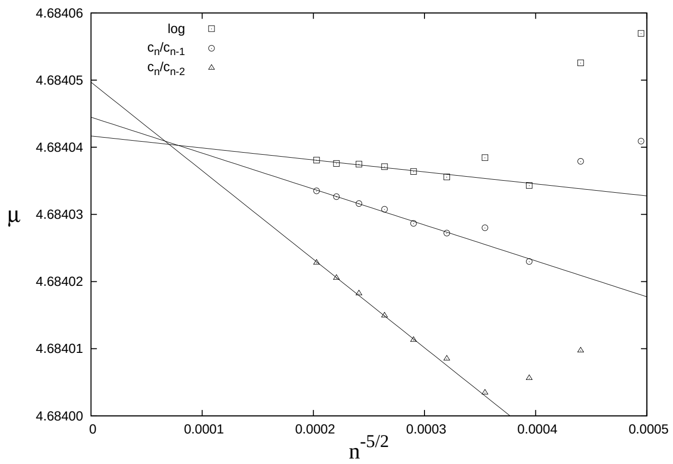

Figure 7. Estimates for μ from $\{q_1, r_2\}$ direct fits.

Table 5. Estimates of μ, γ, and A from direct fits.

Highest	$\log c_n$			c_n/c_{n-1}		c_n/c_{n-2}	
order terms	μ	γ	A	μ	γ	μ	γ
$\{r_0\}$	4.6838981	1.16173	1.18603	4.6839027	1.16166	4.6839099	1.16147
$\{q_0, r_1\}$	4.6840363	1.15708	1.21513	4.6840307	1.15734	4.6840191	1.15789
$\{q_1, r_2\}$	4.6840417	1.15679	1.21708	4.6840444	1.15661	4.6840496	1.15629

relationship between γ and μ, shown in Fig. 10. Note that the biased estimates for the different asymptotic forms are much closer together than the corresponding unbiased

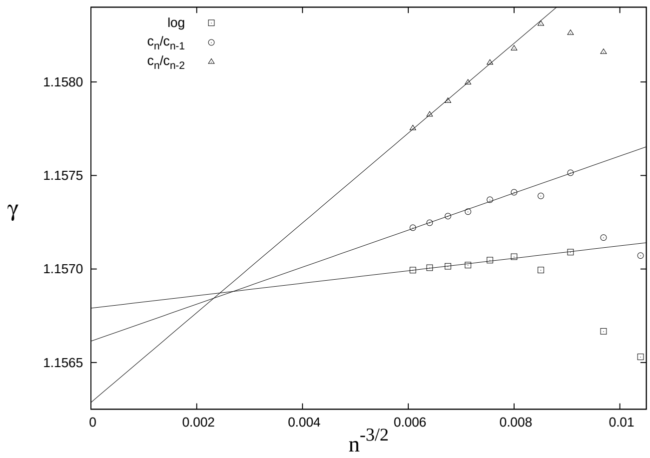

Figure 8. Estimates for γ from $\{q_1, r_2\}$ direct fits.

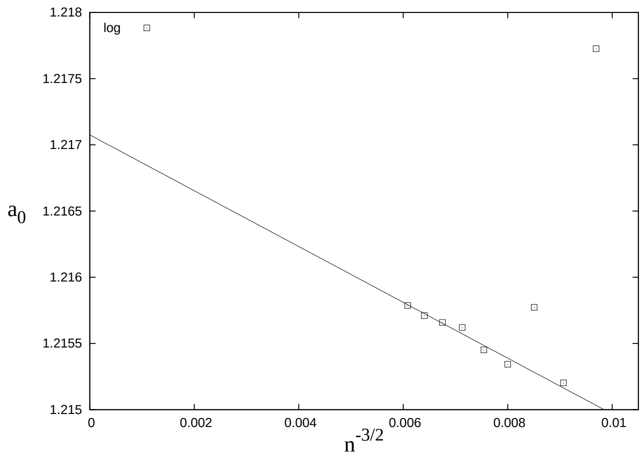

Figure 9. Estimate for the amplitude A from $\{q_1, r_2\}$ direct fit of $\log c_n$.

estimates. Ignoring the small amount of scatter between the different estimates at fixed μ we can draw a sensible line of best fit and convert the range of estimates for μ of $4.684033 \leq \mu \leq 4.684053$ to a corresponding range for γ of $1.1561 \leq \gamma \leq 1.1571$. This agrees very closely with the results of Table 13.

6.1.2. Analyses of the series ρ_n and $\bar{\rho}_n$. We used differential approximants and direct fitting. The Zinn-Justin method was not found to produce useful numerical results in the analysis of $\bar{\rho}_n$, because it does not utilize the fact that $z_c = 1$ is known exactly. We again assume first that $\theta = 0.5$, and consider the effect of possible variation in the value of θ afterward.

The method of differential approximants. We first applied the method of differential approximants to the ρ_n series, and as for the c_n series we find that the resulting estimates

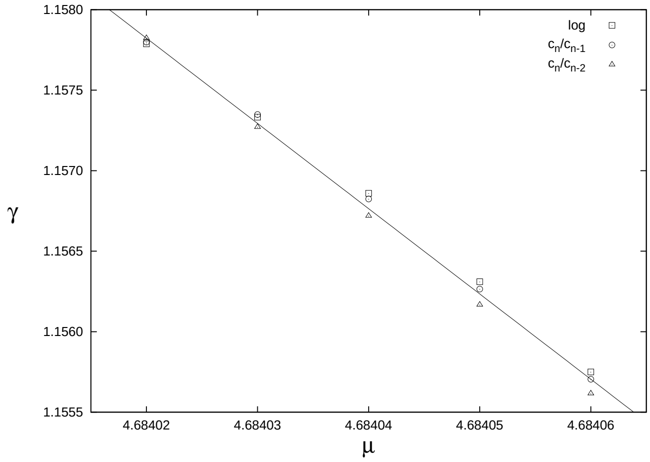

Figure 10. Estimates of γ for biased values of μ from $\{q_1, r_2\}$ direct fits. Line acts as a guide for the eye only.

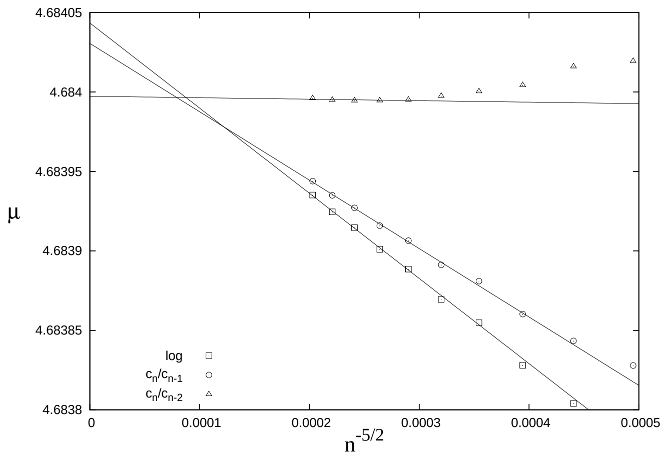

Figure 11. Estimates for μ from $\{q_1, r_1\}$ direct fits of ρ_n series.

are still undergoing large systematic shifts. Indeed the estimates are still some way from the expected value of $\mu \approx 4.684043$, suggesting that confluent corrections are larger for the ρ_n series. The analysis of the $\bar{\rho}_n$ series is more fruitful since we can bias for the known value $z_c = 1$, and easier to interpret because we calculate ν directly rather than $\gamma + 2\nu$.

We first applied the method of differential approximants biased for $z_c = 1$ to the $\bar{\rho}_n$ series, and report the results in Table 6. We see that the estimates are still undergoing large systematic shifts and are a long way from the Monte Carlo and field theory estimates (see Section 7.1). When we bias for the confluent exponent of $\theta = 0.5$ in Table 7 we find much better agreement, and apparently striking convergence to the value of $\nu = 0.58743$ from the second-order differential approximants. We take $\nu = 0.5874$ as our central estimate from the differential approximant analysis, with no estimated

Table 6. Biased differential approximants for $\bar{\rho}_n$.

	Second-order DA		Third-order DA	
N	ν	U/T	ν	U/T
21	0.5933(28)	35/42	0.5922(81)	46/46
22	0.59212(99)	38/43	0.5908(35)	51/58
23	0.59230(63)	43/44	0.59192(46)	63/68
24	0.59207(35)	41/45	0.59212(38)	70/78
25	0.59191(39)	36/44	0.59181(17)	75/90
26	0.591579(94)	36/44	0.59146(32)	93/99
27	0.59138(32)	44/45	0.59158(75)	100/104
28	0.5910(17)	42/44	0.59103(91)	98/107
29	0.59080(45)	40/44	0.5901(11)	108/113
30	0.59092(59)	41/45	0.59058(88)	110/116

Table 7. Differential approximants for $\bar{\rho}_n$, with $\theta = 0.5$.

	Second-order DA		Third-order DA	
N	ν	U/T	ν	U/T
21	0.5893(23)	35/42	0.5850(22)	32/33
22	0.5881(14)	36/43	0.5861(14)	40/46
23	0.58768(93)	38/44	0.58582(52)	50/58
24	0.58805(40)	40/45	0.5857(15)	58/68
25	0.58776(45)	43/44	0.5881(40)	74/78
26	0.58761(18)	39/44	0.58724(87)	78/90
27	0.58747(21)	43/45	0.58698(58)	93/99
28	0.58743(42)	44/44	0.58702(66)	98/104
29	0.587433(91)	42/44	0.58725(40)	90/107
30	0.587434(90)	43/45	0.58756(32)	105/113

range because we cannot anticipate higher-order systematic shifts.

We found that the majority of the second-order approximants and many of the third-order approximants which do not allow for a confluent correction are defective due to singularities on the positive axis in the vicinity of the critical point. In contrast, relatively few of the approximants with a biased confluent exponent are defective.

The method of direct fitting. Direct fits for ρ_n are useful for confirming our previous estimates for μ as shown graphically in Fig. 11, and directly estimating the amplitude

Table 8. Coefficients in asymptotic expansion of $\log \bar{\rho}_n$ with $\theta = 0.5$.

N	ν	D	q_0	q_1	q_2	r_0	r_1	r_2
21	0.58727	1.22663	-0.3628	-0.1352	-0.3395	0.0645	0.0289	-0.0268
22	0.58738	1.22488	-0.3571	-0.1475	-0.3277	0.0646	0.0278	-0.0246
23	0.58748	1.22330	-0.3522	-0.1579	-0.3179	0.0647	0.0267	-0.0222
24	0.58747	1.22336	-0.3523	-0.1579	-0.3178	0.0648	0.0261	-0.0208
25	0.58750	1.22290	-0.3508	-0.1612	-0.3146	0.0648	0.0257	-0.0198
26	0.58750	1.22294	-0.3509	-0.1609	-0.3148	0.0649	0.0254	-0.0191
27	0.58750	1.22296	-0.3510	-0.1607	-0.3151	0.0649	0.0251	-0.0184
28	0.58750	1.22293	-0.3509	-0.1610	-0.3146	0.0649	0.0248	-0.0177
29	0.58750	1.22293	-0.3509	-0.1610	-0.3148	0.0650	0.0245	-0.0169
30	0.58750	1.22292	-0.3508	-0.1612	-0.3145	0.0650	0.0241	-0.0161

Table 9. Coefficients in asymptotic expansion of $\bar{\rho}_n/\bar{\rho}_{n-1}$ with $\theta = 0.5$.

N	ν	q_0	q_1	q_2	r_0	r_1	r_2
21	0.58730	0.1802	0.1884	0.5438	0.1303	0.0420	0.0126
22	0.58741	0.1773	0.2007	0.5268	0.1304	0.0413	0.0141
23	0.58750	0.1751	0.2098	0.5140	0.1305	0.0402	0.0163
24	0.58750	0.1750	0.2103	0.5132	0.1306	0.0400	0.0168
25	0.58752	0.1744	0.2129	0.5093	0.1306	0.0400	0.0169
26	0.58753	0.1744	0.2130	0.5092	0.1306	0.0401	0.0165
27	0.58752	0.1745	0.2123	0.5102	0.1305	0.0402	0.0163
28	0.58752	0.1744	0.2128	0.5094	0.1305	0.0402	0.0163
29	0.58752	0.1745	0.2124	0.5102	0.1306	0.0402	0.0165
30	0.58752	0.1745	0.2126	0.5097	0.1306	0.0400	0.0168

d_0 in Table 11.

For $\bar{\rho}_n$, we found that the highest-order fit with smoothly changing values is $\{q_2, r_2\}$ — biasing the critical point has allowed us to smoothly fit an additional term in the ferromagnetic series, compared to the direct fits of the c_n series. We show the highest-order fits for $\bar{\rho}_n$ in Tables 8–10, in which all coefficients are very stable over the full range of n. In Table 11 we observe rapid convergence for ν as the order of the fit is increased. We use all of the fits and follow the procedure of Section 5.3 to obtain the estimates in Table 13 for ν and D. We may also multiply the upper and lower bounds of the estimates for A and D to obtain an estimate of $AD = 1.4883(60)$, which is compatible with, but more accurate than, the direct estimate from the $\{q_1, r_1\}$ fit of the ρ_n series

Table 10. Coefficients in asymptotic expansion of $\bar{\rho}_n/\bar{\rho}_{n-2}$ with $\theta = 0.5$.

N	ν	q_0	q_1	q_2	r_0	r_1	r_2
21	0.58756	0.3467	0.6716	1.1038	-0.2605	-0.0202	0.0328
22	0.58738	0.3553	0.6377	1.1482	-0.2491	-0.1113	0.2148
23	0.58748	0.3502	0.6592	1.1185	-0.2486	-0.1150	0.2214
24	0.58753	0.3478	0.6694	1.1041	-0.2503	-0.1007	0.1913
25	0.58754	0.3470	0.6727	1.0991	-0.2506	-0.0975	0.1842
26	0.58755	0.3463	0.6757	1.0948	-0.2511	-0.0937	0.1758
27	0.58755	0.3464	0.6753	1.0954	-0.2508	-0.0956	0.1802
28	0.58755	0.3465	0.6751	1.0956	-0.2506	-0.0979	0.1856
29	0.58755	0.3465	0.6751	1.0957	-0.2504	-0.0999	0.1904
30	0.58755	0.3465	0.6747	1.0963	-0.2503	-0.1012	0.1936

Table 11. Estimates of ν, D, and d_0 from direct fits with $\theta = 0.5$.

Highest	$\log \rho_n$	$\log \bar{\rho}_n$		$\bar{\rho}_n/\bar{\rho}_{n-1}$	$\bar{\rho}_n/\bar{\rho}_{n-2}$
order terms	d_0	ν	D	ν	ν
$\{q_0, r_0\}$	1.42961	0.58875	1.20217	0.58878	0.58871
$\{q_1, r_1\}$	1.47943	0.58754	1.21991	0.58761	0.58778
$\{q_2, r_2\}$		0.58751	1.22282	0.58752	0.58754

of 1.4794.

6.1.3. Analysis of the series p_{2n}. The series for p_{2n} is only half as long as the series for c_n and ρ_n. For $d = 2$, there is the advantage that non-analytic corrections to scaling fold into the analytic background term, thus resulting in a particularly simple asymptotic form [40]. No such simplification occurs for $d = 3$, although it does appear from the direct fits that the non-analytic confluent correction terms have small coefficients.

We first apply the method of differential approximants; with a short series the best results are obtained with first-order approximants. These approximants give estimates for μ^2 and α which have large error bars and are not enlightening. If instead we bias the critical point, we obtain quite tight results for α as shown in Table 12. Indeed, with values for μ in quite a large range it seems that the estimates for α are settling down to a value of 0.232. If taken at face value, this would imply that hyperscaling is violated, i.e. $d\nu \neq 2 - \alpha$. However, as was seen in the analysis for the c_n, ρ_n, and $\bar{\rho}_n$ series, it is clear that misleading conclusions can be drawn if the effect of confluent corrections are not factored in. It is difficult to do so with such a short series.

Table 12. Biased estimates for α from first-order DA.

	$\mu = 4.68402$		$\mu = 4.68404$		$\mu = 4.68406$	
N	α	U/T	α	U/T	α	U/T
24	0.242(28)	10/10	0.241(28)	10/10	0.241(28)	10/10
26	0.230(11)	13/13	0.229(11)	13/13	0.229(11)	13/13
28	0.2325(16)	13/14	0.2321(16)	13/14	0.2317(16)	13/14
30	0.23251(56)	15/15	0.23208(54)	15/15	0.23166(53)	15/15
32	0.23251(18)	15/15	0.23202(16)	15/15	0.23153(13)	15/15

Table 13. Estimates of parameters for $d = 3$ from direct fits with $\theta = 0.5$. These are intermediate results which do not yet take into account variation in θ, a dominant source of uncertainty.

μ	γ	ν	A	D
4.6840431(96)	1.15670(51)	0.58752(12)	1.2171(20)	1.2228(29)

Direct fits are also not revealing: it is not possible to get good unbiased estimates of μ^2 and α; when a biased value of μ is used it is possible to fit for a confluent correction with exponent θ, and an analytic correction, but the convergence is not very good and we do not quote these results here. They suggest that α is in the range of $0.23 - 0.24$, consistent with hyperscaling, but without a longer series not much more can be said with confidence.

6.1.4. Effect of variation in θ. Table 31 of [55] reports a wide range of estimates for θ, from a low of 0.46–0.50 from various field theory estimates, to a high of 0.56(3) from the Monte Carlo estimate of [45]. It is therefore important that we repeat the above analysis to quantify the dependence on θ of our estimates for μ, γ, A, ν, D.

The results for μ, γ, ν are shown in Figs. 12–14, with the central estimates given the label 'Best'. It is apparent from the figures that the estimates depend approximately linearly on the value of θ used, and we observed similar linear behavior for A and D. Our method of producing error estimates gives comparable results as θ is varied, and given that this error estimate is subjective in any case we take the uncertainties to be constant. The results can be succinctly summarized by the linear least squares fits to the central estimates:

$$\mu(\theta) = 4.6840431 - 0.0000394(\theta - 0.5) \pm 0.00001 \tag{71}$$

$$\gamma(\theta) = 1.156690 + 0.006779(\theta - 0.5) \pm 0.0005 \tag{72}$$

$$A(\theta) = 1.21723 - 0.06379(\theta - 0.5) \pm 0.002 \tag{73}$$

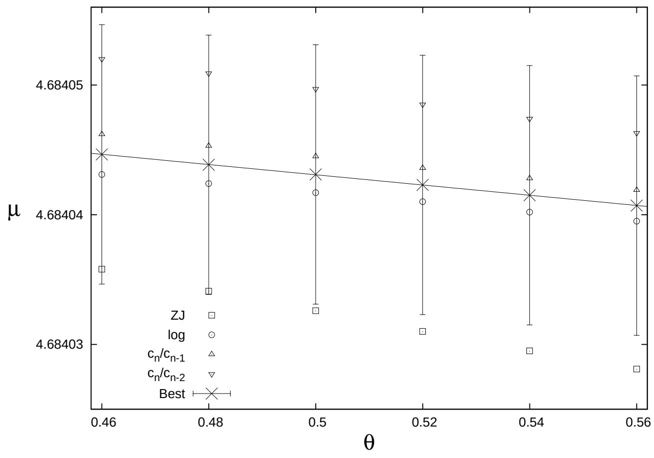

Figure 12. Estimates for μ from $\{q_1, r_2\}$ direct fits and the method of Zinn-Justin, plotted versus θ. Line of best fit to the central estimates ('Best') is also shown.

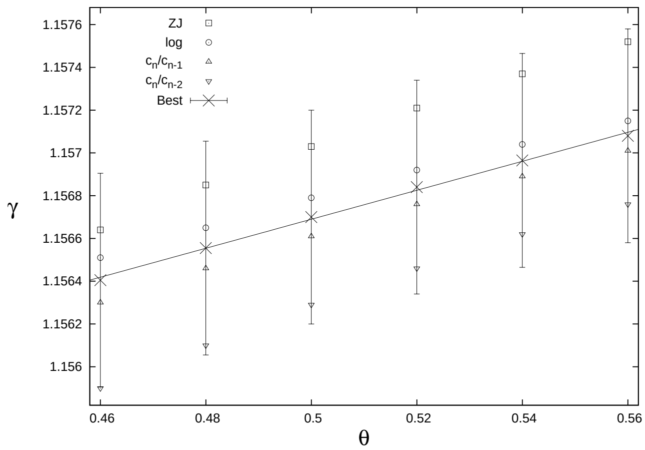

Figure 13. Estimates for γ from $\{q_1, r_2\}$ direct fits and the method of Zinn-Justin, plotted versus θ. Line of best fit to the central estimates ('Best') is also shown.

$$\nu(\theta) = 0.587506 + 0.008324(\theta - 0.5) \pm 0.00012 \tag{74}$$

$$D(\theta) = 1.22330 - 0.19743(\theta - 0.5) \pm 0.003. \tag{75}$$

We show these lines on Figs. 12–14, and it is clear that the fit is excellent in each case. If we adopt a range of $\theta_1 \leq \theta \leq \theta_2$, we then convert this to a range, e.g., for μ of $\mu(\theta_2) - 0.00001 \leq \mu \leq \mu(\theta_1) + 0.00001$.

We note in passing that the 'shift' δn is insensitive to changes in θ, for example in the fit for $\log c_n$ with corrections to order $1/n$, δn only changes from 0.709 to 0.715 as θ is varied from 0.47 to 0.53. For this reason we can use a single value of δn.

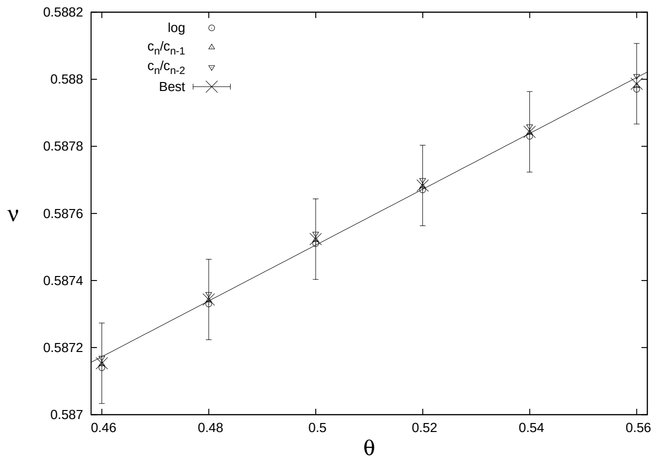

Figure 14. Estimates for ν from $\{q_2, r_2\}$ fits plotted versus θ. Line of best fit to the central estimates ('Best') is also shown.

6.2. Analysis for $d = 4$

The series in $d = 4$ require particular attention because of the logarithmic corrections:

$$c_n \sim A\mu^n (\log n)^{1/4}, \quad \bar{\rho}_n \sim Dn(\log n)^{1/4}. \tag{76}$$

Confluent corrections of the form $\log\log n/\log n$ have been elucidated by Duplantier [13].

The method of differential approximants. Unbiased differential approximants cannot take into account the logarithmic confluent correction, but nevertheless give useful estimates. Second- and third-order inhomogeneous approximants give $\mu = 6.7737 \uparrow$ (trending upwards), and $\gamma = 1.046 \downarrow$ (trending downwards). Biasing $\gamma = 1$ by performing a linear fit in the plot of z_c versus γ, as described below Eqn. (57), gives worse results, suggesting $\mu = 6.777 \downarrow$; this is probably because the unbiased approximants take into account the leading logarithmic correction via an effective exponent. Nonetheless, it appears that the unbiased and biased estimates bracket the correct value of μ (we find this to be the case for dimensions $4 \leq d \leq 7$), and so we take the mean and estimate the uncertainty from the spread of the two estimates.

The method of Zinn-Justin. Naive application of this method, which does not take into account the logarithmic confluent correction, gives $\mu = 6.77363 \uparrow$ if we take $\theta = 1$ as indicated by the direct fits.

The method of direct fitting. Direct fitting works extremely well when the logarithmic correction is taken into account. This results, for example, in a $\log\log$ term for the $\log c_n$ fitting form, and works much better when treated as an effective exponent, rather than biased to have a coefficient of $1/4$. The effective exponent of $\log n$ from the fits for c_n was 0.213, while from the fits for $\bar{\rho}_n$ we obtain 0.326.

It was found that including the explicit $\log\log n/\log n$ correction did not improve the quality of the fits (Grassberger *et al.* [20] do take this correction into account in their Monte Carlo work). For the correction to scaling exponent, the fits make it clear that $\theta \neq 0.5$, and taking $\theta = 1$ gives excellent fits. We take the next correction for the ferromagnetic part to be $O(1/n^2)$; using a correction of $O(1/n^{3/2})$ results in fits which are almost as stable, and yields similar estimates. For the anti-ferromagnetic part we assume that corrections are in increments of 0.5. This assumption results in very acceptable fits for the coefficients in the anti-ferromagnetic part, but it is also true that the estimates we are interested in are essentially the same for *any* reasonable choice of asymptotic form because the ferromagnetic singularity dominates. We use $\{q_1, r_3\}$ and $\{q_2, r_3\}$ fits for c_n, $\{q_1, r_2\}$ and $\{q_2, r_3\}$ fits for $\bar{\rho}_n$.

We do not have much confidence in our estimates for A and D due to the difficulty of distinguishing the constant term from the $\log\log$ term for $\log c_n$, and the possibility of sub-dominant logarithmic corrections which are not accounted for by the asymptotic form.

6.3. Analysis for $d > 4$.

For $d > 4$, the results of [34] provide rigorous proof that for finite-range spread-out models $c_n = A\mu^n[1 + O(n^{-(d-4)/2})]$ and $\bar{\rho}_n = Dn[1 + O(n^{\delta})]$ for any $\delta < \min\{1, \frac{d-4}{2}\}$. The $n^{-(d-4)/2}$ correction to scaling for c_n was first predicted by Guttmann [24] via a renormalisation group argument. We assume that universality holds and use $\theta = \frac{d-4}{2}$ for c_n and $\theta = \min\{1, \frac{d-4}{2}\}$ for $\bar{\rho}_n$ (for $d = 6$, we find evidence of a logarithmic correction for $\bar{\rho}_n$). Further corrections in increments of 0.5 are used, and result in extremely stable fits in all dimensions. For the anti-ferromagnetic term we take the leading correction as $\theta = 0.5$, with further corrections in increments of 0.5. This results in stable estimates for the anti-ferromagnetic coefficients, but it should be noted that the choice of fitting form for the anti-ferromagnetic part is not crucial as estimates for μ, A, and D are quite insensitive to this choice.

Our analysis follows the broad outlines discussed above for $d = 3, 4$, and below we mention some key points for each dimension. Our results are summarized in Table 15.

$d = 5$. Differential approximant analyses of the $\bar{\rho}_n$ series provide convincing numerical evidence that $\theta = 0.5$. Direct fits and the method of Zinn-Justin confirm $\theta = 0.5$ for both c_n and $\bar{\rho}_n$. We use $\{q_1, r_1\}$ and $\{q_2, r_2\}$ fits for c_n, $\{q_2, r_2\}$ and $\{q_3, r_2\}$ fits for $\bar{\rho}_n$.

$d = 6$. For the method of Zinn-Justin we obtain good results using $\theta = 1$. The direct fits confirm that the leading correction for c_n does not include a $\log n/n$ term. For $\bar{\rho}_n$, the direct fits give evidence of $\log n/n$ and $1/n$ corrections, but we only fit the dominant

$\log n/n$ part as the fit is not improved when $1/n$ is included. For c_n we use $\{q_1, r_1\}$ and $\{q_2, r_2\}$ fits, while for $\bar{\rho}_n$ we use $\{q_2, r_1\}$ and $\{q_3, r_2\}$ fits.

$d = 7$. The direct fits and the method of Zinn-Justin confirm the absence of a $1/n$ term for c_n, and the presence of this term for $\bar{\rho}_n$. For c_n we use $\{q_1, r_1\}$ and $\{q_2, r_2\}$ fits, while for $\bar{\rho}_n$ we use $\{q_2, r_1\}$ and $\{q_3, r_2\}$ fits.

$d = 8$. Biased and unbiased differential approximant estimates no longer bracketed the accurate Monte Carlo estimate for μ [54]. Biasing the exponent as discussed below Eqn. (57) gave estimates that were far more stable and hence these were used to obtain the central estimate and uncertainty. Direct fits and the method of Zinn-Justin clearly confirm that the leading correction is $1/n^2$ for c_n. Direct fits show the presence of the $1/n$ term for $\bar{\rho}_n$; from the fits nothing definitive can be said as to the nature of the next correction, and in particular could not distinguish between $\log n/n^2$ and $1/n^2$ corrections. We used $1/n^2$, but the two choices gave very similar numerical results. For c_n we use $\{q_1, r_1\}$ and $\{q_2, r_2\}$ fits, while for $\bar{\rho}_n$ we use $\{q_2, r_1\}$ and $\{q_3, r_2\}$ fits.

6.4. Analysis of the $1/d$ series

We obtain estimates from the $1/d$ expansions of Eqns. (1), (3), and (4), via truncation and Padé-Borel resummation [43]. We found that changing the expansion variable to $2d - 1$, as appears, e.g., in Fisher and Gaunt [14], makes no appreciable difference for either method.

For truncation, we have used the rule of thumb that an asymptotic series should be truncated before its smallest term and then half of the smallest term should be added, or all terms should be utilized if they decrease uniformly; we do not take these values very seriously. For Padé-Borel estimates we use diagonal Padé approximants, and Cauchy principal value integration when there are spurious singularities on the positive real axis. The uncertainties were obtained by subjective consideration of the spread of estimates.

7. Analysis of series: conclusions

7.1. Estimates of critical parameters

Our results are summarized in Tables 14–15.

Error estimation. To quote Guttmann [26] on error estimation in series analysis, "The question of error estimates is a vexed one." Also, "error bounds are generally referred to as (subjective) confidence limits, and as such frequently measure the enthusiasm of the author rather than the quality of the data." We are only too aware of the fact that the estimation of errors in our analysis is not a rigorous science, and have tried to temper our enthusiasm. There is little doubt that our $n \leq 30$ series for $d = 3$ have still not reached their asymptotic regimes, and our analyses may very well still be subject to unknown systematic shifts — our situation is far from the luxury of the long series available for the square lattice [40, 41].

We have already discussed our method of error estimation for direct fits, at the end of Section 5.3. To reiterate, for the direct fits the values in parentheses are not statistical error estimates and should not be read as such. For the c_n fits, the central value is the mean of the $\log c_n$, c_n/c_{n-1}, and c_n/c_{n-2} fits (except for $d = 3$ where we disregard the c_n/c_{n-2} fit), and the value in parentheses is the mean of the jumps from the second highest-order fit to the highest-order fit. This is a purely mechanical process, which has the significant advantage that it is independent of the enthusiasm of the author, but we stress that it does not provide statistical error estimates. The degree to which these estimates represent the true error depends upon the nature and size of higher-order corrections which *are not* and *cannot be* taken into account. *If* these corrections are small, then the values in parentheses give some idea of the accuracy of the estimate.

For the differential approximant estimates in dimensions $4 \leq d \leq 7$ we find the mean value of the estimates for μ from the highest-order approximants (those utilizing at least $c_0, \ldots, c_{22}$). We also bias the approximant estimates by performing a linear fit of the scatter plot of γ versus z_c for the highest-order approximants, and taking the intercept of this line with $\gamma = 1$. For these dimensions the unbiased and biased estimates both have uniform trends as the order of the approximants are increased, and appear to be pinching the correct value for μ. Hence we take the mean of the unbiased and biased estimates as our central estimate, and half the difference is the spread which we give in parentheses. For $d = 8$ the trend from the unbiased estimates is less clear, and instead we take the biased estimates, with the value in parentheses a subjective estimate of the spread of the highest-order biased estimates.

$d = 3$. The study of self-avoiding walks in the three dimensions via direct enumeration and Monte Carlo methods has a long history, with an equally long history of underestimation of systematic shifts and hence underestimation of errors in the estimates of critical points and critical exponents. Much of that history is documented by Li *et al.* [45] and Pelissetto and Vicari [55]. We compare our results with recent results from direct enumeration, Monte Carlo and field theory methods in Table 14.

Our results are reported using the two possible ranges $0.47 \leq \theta \leq 0.5$ and $0.47 \leq \theta \leq 0.56$. The smaller range is based on field theory estimates reported in Table 31 of [55]. The larger range encompasses also the mid-value of the Monte Carlo estimate $\theta = 0.56(3)$ of [45]; the authors of [45] observe that their estimate may actually be for an effective exponent influenced by higher-order corrections. Other scenarios for the value of θ can easily be converted to ranges of estimates via Eqns. (72)–(75).

The most recent enumeration work by MacDonald *et al.* [47] gives an estimate $\gamma = 1.1585$, but cannot rule out γ being elsewhere in the range $1.155 \leq \gamma \leq 1.160$. They place considerably tighter bounds upon ν, with estimates in the range of $0.5870 \leq \nu \leq 0.5881$; we have reported the midpoint in Table 14.

It is apparent from Table 14 that the estimates for μ have an upward trend as more

Table 14. Estimates of parameters for $d = 3$. Our direct fit estimates using c_n and $\bar{\rho}_n$ with $n \leq 30$ are reported in the top two lines.

	μ	γ	ν	A	D
$0.47 \leq \theta \leq 0.5$	4.684044(11)	1.1566(6)	0.5874(2)	1.218(3)	1.226(6)
$0.47 \leq \theta \leq 0.56$	4.684043(12)	1.1568(8)	0.5876(5)	1.216(5)	1.220(12)
[47] $n \leq 26$ (2000)	4.68404(9)	1.1585	0.58755	1.205	1.225
[46] $n \leq 23$ (1992)	4.683869(22)	1.16193(10)			
[27] $n \leq 21$ (1989)	4.68393(9)	1.161(2)	0.592(3)		
[36] MC (2004)	4.684038(6)				
[37] MC (2004)		1.1573(2)			
[57] MC (2001)			0.5874(2)		
[6] MC (1998)		1.1575(6)			
[2] MC (1997)			0.58756(5)		
[45] MC (1995)			0.5877(6)		
[21] FT $d = 3$ (1998)		1.1596(20)	0.5882(11)		
[21] FT ϵ (1998)		1.1575(60)	0.5875(25)		
[21] FT ϵ bc (1998)		1.1571(30)	0.5878(11)		

terms have been added to the series. For γ, earlier estimates from direct enumeration are systematically lower than recent estimates from all sources. A similar trend can be seen in Table 31 of [55] for the Monte Carlo estimates of ν. This is because earlier analyses neglected the effect of the leading confluent correction, which resulted in systematic errors in the central estimates. On some occasions the apparent convergence of one method of series analysis or another also resulted in overly-optimistic confidence limits.

Our estimate for μ is far more accurate than that from previous enumeration work, and given that the variance with θ is slight, we adopt the estimate $\mu = 4.684043(12)$ ($0.47 \leq \theta \leq 0.56$) as our final value. Our value of μ is consistent with the Monte Carlo estimate given in [36]. For the exponents γ and ν our analysis complements and confirms recent Monte Carlo and field theory estimates. Our estimates are perhaps of comparable accuracy to the Monte Carlo estimates, but without the rigor of a statistical error estimate. For this reason we would give the best available Monte Carlo estimates more weight, but our analysis suggests that γ may well be on the low side of the Monte Carlo range. For ν our estimate is in accordance with all of the recent Monte Carlo and field theory estimates.

$d \geq 4$. Our conclusions for $d \geq 4$ are tabulated in Table 15. Our best results come from the direct fits and for $d \geq 5$ these agree with the careful Monte Carlo work of Owczarek and Prellberg [54]. The direct fit estimates for $d = 4$ are heavily influenced by the logarithmic correction and the inability to effectively take into account sub-dominant logarithmic terms. The accuracy of the series analysis estimate of μ for $d = 4$ has improved significantly since the estimate $\mu = 6.7720(5)$ found 30 years ago by

Table 15. Estimates of parameters for $d \geq 4$. We use 'OP' to indicate Monte Carlo results of Owczarek and Prellberg [54], 'DA' for the method of differential approximants, 'ZJ' for the method of Zinn-Justin, 'direct' for the method of direct fitting, '$1/d$ T' for the truncated $1/d$ expansion, and '$1/d$ PB' for the $1/d$ Padé-Borel method. Entries without error indications have large uncertainties.

	$d = 4$	$d = 5$	$d = 6$	$d = 7$	$d = 8$
μ (OP)	6.774043(5)	8.838544(3)	10.878094(4)	12.902817(3)	14.919257(2)
μ (DA)	6.7752(16)	8.83856(21)	10.878086(12)	12.902828(16)	14.919255(5)
μ (ZJ)	6.77363 $\uparrow$	8.83872 $\downarrow$	10.878134 $\downarrow$	12.902828 $\downarrow$	14.919261 $\downarrow$
μ (direct)	6.774168(32)	8.8385451(90)	10.8780919(21)	12.9028174(53)	14.9192552(11)
μ ($1/d$ T)	6.687	8.823	10.8749	12.90207	14.919095
μ ($1/d$ PB)	6.78(1)	8.837(3)	10.8775(20)	12.9028(2)	14.91925(10)
A (direct)	1.107	1.2770(2)	1.15894(1)	1.11418(4)	1.090441(4)
A ($1/d$ T)	–	1.2045	1.1665	1.1154	1.09067
A ($1/d$ PB)	–	1.231(3)	1.1537(10)	1.11362(15)	1.09410(15)
D (OP)	–	1.4767(13)	1.2940(6)	1.2187(3)	1.1760(2)
D (direct)	1.035	1.47722(8)	1.29452(4)	1.21878(1)	1.176177(5)
D ($1/d$ T)	–	1.3839	1.30276	1.220148	1.17643
D ($1/d$ PB)	–	1.42(1)	1.288(2)	1.2180(5)	1.1761(1)

Guttmann [23], due to the availability of additional coefficients (see also [46] for more recent work).

7.2. Rigorous bounds on the connective constant

It is proved in [1] that μ is bounded above by the unique positive root of

$$2dx^{n-1} = (c_n - (2d-2)c_{n-1})\,x + (2d-2)\left((2d-1)c_{n-1} - c_n\right). \tag{77}$$

The bounds we obtain from this are 4.7552, 6.8251, 8.8671, 10.8949, 12.9137, 14.9270, 16.9368, 18.9443, 20.9502, 22.9549, starting from $d = 3$, all rounded up. These are not as good as the upper bounds 4.7387, 6.8179, 8.8602, 10.8886 for dimensions $d = 3, 4, 5, 6$ [53, 56]. It is erroneously claimed in [47] that c_{26} gives $\mu \leq 4.7114$ for $d = 3$; in fact c_{26} gives the weaker bound $\mu \leq 4.7626$ using (77). For rigorous lower bounds, see [12, 33, 58].

A. Appendix: Enumeration tables

The following tables give the results of our enumerations of $\pi_{m,\delta}$, $r_{m,\delta}$, c_n, ρ_n and p_n. See [9] for more extensive tables, also in machine-readable form.

Table 16. $\pi_{m,\delta}$

m	$\delta=2$	$\delta=3$	$\delta=4$	$\delta=5$	$\delta=6$	$\delta=7$
4	-1	0	0	0	0	0
5	3	0	0	0	0	0
6	-8	-4	0	0	0	0
7	19	15	0	0	0	0
8	-50	-86	-27	0	0	0
9	121	300	106	0	0	0
10	- 305	-1 511	-1 340	- 248	0	0
11	736	5 297	5 333	966	0	0
12	-1 853	-25 566	-52 252	-25 020	-2 830	0
13	4 531	91 234	211 403	100 988	10 755	0
14	-11 444	- 435 330	-1 907 566	-1 850 364	- 515 509	-38 232
15	28 294	1 586 306	7 854 601	7 635 822	2 029 500	141 271
16	-71 803	-7 568 792	-68 777 498	- 123 248 980	-64 816 437	-11 448 832
17	179 006	28 105 857	288 074 727	517 006 517	260 695 401	43 562 781
18	- 455 588	- 134 512 520	-2 498 227 824	-7 899 351 270	-7 074 329 136	-2 259 048 705
19	1 142 357	507 675 751	10 626 960 167	33 569 520 427	28 860 719 280	8 752 861 880
20	-2 914 236	-2 438 375 322	-92 047 793 514	- 500 752 577 733	- 724 291 034 691	- 375 104 500 306
21	7 341 457	9 330 924 963	396 919 882 288	2 150 581 793 271	2 984 307 507 943	1 470 382 570 259
22	-18 768 621	-44 965 008 206	-3 445 692 397 195	-31 789 616 257 271	-72 005 867 458 629	-57 134 966 511 160
23	47 466 002	174 103 216 625	15 035 569 992 917	137 713 940 393 321	298 797 296 949 195	225 664 948 525 652
24	- 121 579 349	- 841 380 441 626	- 130 974 140 581 412	-2 032 548 406 479 564	-7 072 798 632 884 530	-8 310 727 395 423 391
25	308 478 355	3 290 830 791 268				
26	- 791 455 148	-15 941 476 401 251				
27	2 013 666 265	62 897 919 980 935				
28	-5 174 044 897	- 305 298 415 550 796				
29	13 195 280 922	1 213 812 491 872 081				
30	-33 949 508 883	-5 901 490 794 431 276				

Table 17. $\pi_{m,\delta}$

m	$\delta=8$	$\delta=9$	$\delta=10$	$\delta=11$	$\delta=12$
16	- 593 859	0	0	0	0
17	2 136 990	0	0	0	0
18	- 272 284 377	-10 401 712	0	0	0
19	1 002 540 792	36 572 274	0	0	0
20	-79 389 607 706	-6 916 928 958	- 202 601 898	0	0
21	296 580 166 041	24 752 523 462	698 531 550	0	0
22	-18 991 828 571 041	-2 845 232 717 076	- 187 336 983 764	-4 342 263 000	0
23	71 607 362 439 324	10 298 433 232 362	654 746 926 835	14 729 974 326	0
24	-4 089 518 594 710 646	- 940 637 759 037 584	- 104 821 777 374 466	-5 399 047 490 020	- 101 551 822 350

Table 18. $r_{m,\delta}$

m	$\delta = 2$	$\delta = 3$	$\delta = 4$	$\delta = 5$	$\delta = 6$	$\delta = 7$
4	0	0	0	0	0	0
5	3	0	0	0	0	0
6	-2	0	0	0	0	0
7	19	15	0	0	0	0
8	-20	-4	0	0	0	0
9	125	298	106	0	0	0
10	- 142	- 116	50	0	0	0
11	756	5 293	5 407	966	0	0
12	- 908	-1 748	2 596	1 092	0	0
13	4 651	92 352	217 915	103 652	10 755	0
14	-5 866	-20 354	131 382	123 752	17 014	0
15	29 298	1 635 204	8 259 099	8 006 364	2 087 098	141 271
16	-38 772	- 151 826	6 388 800	10 689 852	3 502 180	259 148
17	187 890	29 528 009	309 549 227	553 251 595	273 897 083	44 651 913
18	- 256 882	1 278 760	296 929 090	833 860 050	497 935 412	86 977 956
19	1 212 409	543 884 539	11 678 266 645	36 649 327 719	30 892 753 566	9 143 099 504
20	-1 697 476	97 253 034	13 365 532 342	61 812 465 594	60 930 016 102	18 995 212 456
21	7 867 353	10 199 601 195	446 192 990 524	2 394 416 093 217	3 249 327 197 509	1 560 447 905 709
22	-11 237 646	3 153 169 354	589 944 786 900	4 460 020 424 324	6 911 804 871 782	3 446 582 798 592
23	51 362 358	194 242 768 721	17 288 192 341 291	156 284 036 525 425	330 519 809 708 571	242 813 958 590 662
24	-74 621 132	84 105 863 986	25 752 215 129 708	317 387 352 958 176	752 352 026 288 734	566 890 329 449 136
25	337 011 419	3 747 592 552 768				
26	- 496 595 594	2 061 502 580 308				
27	2 220 181 989	73 105 694 028 337				
28	-3 311 032 564	48 288 532 248 224				
29	14 677 154 178	1 439 625 055 822 687				
30	-22 116 633 042	1 100 771 160 651 506				

Table 19. $r_{m,\delta}$

m	$\delta = 8$	$\delta = 9$	$\delta = 10$	$\delta = 11$	$\delta = 12$
16	0	0	0	0	0
17	2 136 990	0	0	0	0
18	4 145 208	0	0	0	0
19	1 022 582 952	36 572 274	0	0	0
20	2 101 078 756	71 405 424	0	0	0
21	307 217 748 067	25 128 377 158	698 531 550	0	0
22	666 147 872 258	51 671 531 788	1 337 713 388	0	0
23	75 123 854 243 770	10 580 731 025 256	662 104 401 197	14 729 974 326	0
24	170 927 657 160 212	22 755 445 969 576	1 325 124 449 256	27 337 708 760	0

Table 20. Enumeration results for $d = 3$

n	p_n	c_n	ρ_n
1	0	6	6
2	0	30	72
3	0	150	582
4	3	726	4 032
5	0	3 534	25 566
6	22	16 926	153 528
7	0	81 390	886 926
8	207	387 966	4 983 456
9	0	1 853 886	27 401 502
10	2 412	8 809 878	148 157 880
11	0	41 934 150	790 096 950
12	31 754	198 842 742	4 166 321 184
13	0	943 974 510	21 760 624 254
14	452 640	4 468 911 678	112 743 796 632
15	0	21 175 146 054	580 052 260 230
16	6 840 774	100 121 875 974	2 966 294 589 312
17	0	473 730 252 102	15 087 996 161 382
18	108 088 232	2 237 723 684 094	76 384 144 381 272
19	0	10 576 033 219 614	385 066 579 325 550
20	1 768 560 270	49 917 327 838 734	1 933 885 653 380 544
21	0	235 710 090 502 158	9 679 153 967 272 734
22	29 764 630 632	1 111 781 983 442 406	48 295 148 145 655 224
23	0	5 245 988 215 191 414	240 292 643 254 616 694
24	512 705 615 350	24 730 180 885 580 790	1 192 504 522 283 625 600
25	0	116 618 841 700 433 358	5 904 015 201 226 909 614
26	9 005 206 632 672	549 493 796 867 100 942	29 166 829 902 019 914 840
27	0	2 589 874 864 863 200 574	143 797 743 705 453 990 030
28	160 810 554 015 408	12 198 184 788 179 866 902	707 626 784 073 985 438 752
29	0	57 466 913 094 951 837 030	3 476 154 136 334 368 955 958
30	2 912 940 755 956 084	270 569 905 525 454 674 614	17 048 697 241 184 582 716 248
32	53 424 552 150 523 386		

Table 21. Enumeration results for $d = 4$

n	p_n	c_n	ρ_n
1	0	8	8
2	0	56	128
3	0	392	1 416
4	6	2 696	13 568
5	0	18 584	119 960
6	76	127 160	1 009 440
7	0	871 256	8 205 656
8	1 434	5 946 200	65 068 352
9	0	40 613 816	506 193 144
10	32 616	276 750 536	3 879 735 776
11	0	1 886 784 200	29 378 067 080
12	844 432	12 843 449 288	220 265 711 040
13	0	87 456 597 656	1 637 726 387 096
14	23 919 864	594 876 193 016	12 091 336 503 584
15	0	4 047 352 264 616	88 727 095 777 896
16	723 317 892	27 514 497 698 984	647 661 676 223 168
17	0	187 083 712 725 224	4 705 654 523 841 704
18	22 985 014 408	1 271 271 096 363 128	34 049 855 885 188 128
19	0	8 639 846 411 760 440	245 482 626 441 965 048
20	759 455 943 180	58 689 235 680 164 600	1 764 039 730 476 165 824
21	0	398 715 967 140 863 864	12 638 999 670 514 091 256
22	25 896 526 976 232	2 707 661 592 937 721 288	90 314 929 495 362 821 216
23	0	18 389 434 921 635 285 800	643 797 168 943 155 174 632
24	906 280 281 013 716	124 852 857 467 211 187 784	4 579 056 522 808 853 475 648
26	32 415 166 885 106 016		

Table 22. Enumeration results for $d = 5$

n	p_n	c_n	ρ_n
1	0	10	10
2	0	90	200
3	0	810	2 810
4	10	7 210	34 400
5	0	64 250	390 250
6	180	570 330	4 224 040
7	0	5 065 530	44 258 330
8	5 170	44 906 970	452 994 880
9	0	398 227 610	4 554 189 370
10	186 856	3 527 691 690	45 150 385 960
11	0	31 255 491 850	442 585 257 210
12	7 762 660	276 741 169 130	4 298 424 239 520
13	0	2 450 591 960 890	41 422 888 065 930
14	355 211 280	21 690 684 337 690	396 562 641 220 520
15	0	192 003 889 675 210	3 775 000 221 446 410
16	17 452 391 500	1 699 056 192 681 930	35 759 109 994 183 040
17	0	15 035 937 610 909 770	337 271 171 816 820 170
18	905 482 413 120	133 030 135 015 071 770	3 168 963 365 639 859 240
19	0	1 177 032 340 670 878 170	29 674 213 141 523 338 410
20	49 043 820 354 532	10 412 322 608 416 261 050	277 027 018 652 760 361 440
21	0	92 113 105 222 899 934 010	2 579 137 185 681 364 258 410
22	2 750 466 599 904 160	814 766 179 787 983 302 090	23 952 499 155 763 685 289 000
23	0	7 207 026 563 685 440 727 850	221 945 733 507 158 827 283 850
24	158 750 348 183 470 420	63 742 525 570 299 581 210 090	2 052 336 893 487 422 784 497 920

Table 23. Enumeration results for $d = 6$

n	p_n	c_n	ρ_n
1	0	12	12
2	0	132	288
3	0	1 452	4 908
4	15	15 852	73 152
5	0	173 172	1 012 980
6	350	1 887 492	13 402 992
7	0	20 578 452	171 862 548
8	13 545	224 138 292	2 154 376 608
9	0	2 441 606 532	26 543 662 692
10	679 716	26 583 605 772	322 653 340 560
11	0	289 455 960 492	3 879 491 118 732
12	39 976 300	3 150 796 704 012	46 230 423 160 608
13	0	34 298 615 880 372	546 792 606 800 628
14	2 617 358 820	373 292 253 262 692	6 426 234 180 376 752
15	0	4 062 873 240 668 412	75 112 752 191 837 340
16	185 273 093 790	44 214 072 776 280 252	873 794 699 391 076 512
17	0	481 167 126 859 845 852	10 122 684 403 923 474 108
18	13 920 089 014 540	5 235 893 033 922 430 692	116 838 193 175 893 802 928
19	0	56 975 931 806 991 140 292	1 344 159 773 521 989 828 132
20	1 096 290 450 188 094	619 957 835 069 070 600 132	15 418 548 294 824 495 850 720
21	0	6 745 858 105 534 183 489 092	176 395 640 689 420 430 956 932
22	89 700 671 592 514 860	73 398 893 398 168 440 782 892	2 013 229 649 322 045 469 598 928
23	0	798 629 075 137 768 054 499 292	22 927 303 036 559 662 145 100 348
24	7 575 158 745 971 797 850	8 689 265 092 167 904 101 731 532	260 584 818 024 344 531 410 575 072

Acknowledgments

NC acknowledges support by the Australian Research Council and the Centre of Excellence for Mathematics and Statistics of Complex Systems. RL acknowledges the support of Postgraduate Scholarships from NSERC of Canada. The work of GS was supported in part by NSERC. We benefited from the Pacific Institute for the Mathematical Sciences 2005 Summer School in Probability, during which we had the opportunity to work together. We thank Tony Guttmann and Andrew Rechnitzer for helpful discussions. All numerical calculations were performed using the computational resources of the Victorian Partnership for Advanced Computing (VPAC).

References

[1] R. Ahlberg and S. Janson. Upper bounds for the connective constant. Unpublished manuscript, (1980).

[2] P. Belohorec. *Renormalization group calculation of the universal critical exponents of a polymer molecule*. PhD thesis, University of Guelph, (1997).

[3] D.C. Brydges and J.Z. Imbrie. End-to-end distance from the Green's function for a hierarchical self-avoiding walk in four dimensions. *Commun. Math. Phys.*, **239**:523–547, (2003).

[4] D.C. Brydges and T. Spencer. Self-avoiding walk in 5 or more dimensions. *Commun. Math. Phys.*, **97**:125–148, (1985).

[5] M. Campostrini, A. Pelissetto, P. Rossi, and E. Vicari. 25th-order high-temperature expansion results for three-dimensional Ising-like systems on the simple-cubic lattice. *Phys. Rev. E*, **65**:066127, (2002).

[6] S. Caracciolo, M.S. Causo, and A. Pelissetto. High-precision determination of the critical exponent γ for self-avoiding walks. *Phys. Rev. E*, **57**:1215–1218, (1998).

[7] S. Caracciolo, A.J. Guttmann, I. Jensen, A. Pelissetto, A.N. Rogers, and A.D. Sokal. Correction to scaling exponents for two-dimensional self-avoiding walks. *J. Statist. Phys.*, **120**:1037–1100, (2005).

[8] M. Chen and K.Y. Lin. Amplitude ratios for self-avoiding walks on hypercubic lattices in 4 to 6 dimensions. *Chinese J. Phys.*, **41**:52–58, (2003).

[9] N. Clisby, R. Liang, and G. Slade. Self-avoiding walk enumeration via the lace expansion: tables. Unpublished, (2007). `http://www.math.ubc.ca/~slade/lacecounts` has enumeration data in machine-readable form.

[10] N. Clisby and G. Slade. In preparation.

[11] A.R. Conway, I.G. Enting, and A.J. Guttmann. Algebraic techniques for enumerating self-avoiding walks on the square lattice. *J. Phys. A: Math. Gen.*, **26**:1519–1534, (1993).

[12] A.R. Conway and A.J. Guttmann. Lower bound on the connective constant for square lattice self-avoiding walks. *J. Phys. A: Math. Gen.*, **26**:3719–3724, (1993).

[13] B. Duplantier. Polymer chains in four dimensions. *Nuclear Physics B*, **275** [FS17]:319–355, (1986).

[14] M.E. Fisher and D.S. Gaunt. Ising model and self-avoiding walks on hypercubical lattices and "high-density" expansions. *Phys. Rev.*, **133**:A224–A239, (1964).

[15] M.E. Fisher and R.R.P. Singh. Critical points, large-dimensionality expansions, and the Ising spin glass. In G.R. Grimmett and D.J.A. Welsh, editors, *Disorder in Physical Systems*. Clarendon Press, Oxford, (1990).

[16] M.E. Fisher and M.F. Sykes. Excluded-volume problem and the Ising model of ferromagnetism. *Phys. Rev.*, **114**:45–58, (1959).

[17] D.S. Gaunt. $1/d$ expansions for critical amplitudes. *J. Phys. A: Math. Gen.*, **19**:L149–L153, (1986).

[18] D.S. Gaunt and A.J. Guttmann. Asymptotic analysis of coefficients. In C. Domb and M.S. Green, editors, *Phase Transitions and Critical Phenomena,* Volume 3, pages 181–243. Academic Press, New York, (1974).

[19] P.R. Gerber and M.E. Fisher. Critical temperatures of classical n-vector models on hypercubic lattices. *Phys. Rev. B*, **10**:4697–4703, (1974).

[20] P. Grassberger, R. Hegger, and L. Schäfer. Self-avoiding walks in four dimensions: logarithmic corrections. *J. Phys. A: Math. Gen.*, **27**:7265–7282, (1994).

[21] R. Guida and J. Zinn-Justin. Critical exponents of the N-vector model. *J. Phys. A: Math. Gen.*, **31**:8103–8121, (1998).

[22] A. J. Guttmann and S. G. Whittington. Two-dimensional lattice embeddings of connected graphs of cyclomatic index two. *J. Phys. A: Math. Gen.*, **11**:721–729, (1978).

[23] A.J. Guttmann. On the zero-field susceptibility in the $d = 4$, $n = 0$ limit: analysing for confluent logarithmic singularities. *J. Phys. A: Math. Gen.*, **11**:L103–L106, (1978).

[24] A.J. Guttmann. Correction to scaling exponents and critical properties of the n-vector model with dimensionality > 4. *J. Phys. A: Math. Gen.*, **14**:233–239, (1981).

[25] A.J. Guttmann. On the critical behaviour of self-avoiding walks. *J. Phys. A: Math. Gen.*, **20**:1839–1854, (1987).

[26] A.J. Guttmann. Asymptotic analysis of power-series expansions. In C. Domb and J.L. Lebowitz, editors, *Phase Transitions and Critical Phenomena,* Volume 13, pages 1–234. Academic Press, New York, (1989).

[27] A.J. Guttmann. On the critical behaviour of self-avoiding walks: II. *J. Phys. A: Math. Gen.*, **22**:2807–2813, (1989).

[28] A.J. Guttmann and J. Wang. The extension of self-avoiding random walk series in two dimensions. *J. Phys. A: Math. Gen.*, **24**:3107–3109, (1991).

[29] J.M. Hammersley and K.W. Morton. Poor man's Monte Carlo. *J. Roy. Stat. Soc. B*, **16**:23–38, (1954).

[30] T. Hara and G. Slade. The lace expansion for self-avoiding walk in five or more dimensions. *Reviews in Math. Phys.*, **4**:235–327, (1992).

[31] T. Hara and G. Slade. Self-avoiding walk in five or more dimensions. I. The critical behaviour. *Commun. Math. Phys.*, **147**:101–136, (1992).

[32] T. Hara and G. Slade. The self-avoiding-walk and percolation critical points in high dimensions. *Combin. Probab. Comput.*, **4**:197–215, (1995).

[33] T. Hara, G. Slade, and A.D. Sokal. New lower bounds on the self-avoiding-walk connective constant. *J. Statist. Phys.*, **72**:479–517, (1993). Erratum: *J. Statist. Phys.*, **78**:1187–1188, (1995).

[34] R. van der Hofstad and G. Slade. The lace expansion on a tree with application to networks of self-avoiding walks. *Adv. Appl. Math.*, **30**:471–528, (2003).

[35] R. van der Hofstad and G. Slade. Expansion in n^{-1} for percolation critical values on the n-cube and $\mathbb{Z}^n$: the first three terms. *Combin. Probab. Comput.*, **15**:695–713, (2006).

[36] H.-P. Hsu and P. Grassberger. Polymers confined between two parallel plane walls. *J. Chem. Phys.*, **120**:2034–2041, (2004).

[37] H.-P. Hsu, W. Nadler, and P. Grassberger. Scaling of star polymers with 1–80 arms. *Macromolecules*, **37**:4658–4663, (2004).

[38] B.D. Hughes. *Random Walks and Random Environments*, volume 1: Random Walks. Oxford University Press, Oxford, (1995).

[39] D.L. Hunter and G.A. Baker Jr. Methods of series analysis. III. Integral approximant methods. *Phys. Rev.*, **B19**:3808–3821, (1979).

[40] I. Jensen. A parallel algorithm for the enumeration of self-avoiding polygons on the square lattice. *J. Phys. A: Math. Gen.*, **36**:5731–5745, (2003).

[41] I. Jensen. Enumeration of self-avoiding walks on the square lattice. *J. Phys. A: Math. Gen.*, **37**:5503–5524, (2004).

[42] H. Kesten. On the number of self-avoiding walks. II. *J. Math. Phys.*, **5**:1128–1137, (1964).

[43] H. Kleinert and V. Schulte-Frohlinde. *Critical Properties of ϕ^4-Theories.* World Scientific, Singapore, (2001).

[44] D.E. Knuth. *The Art of Computer Programming,* Volume 3. Addison Wesley, Reading, (1973).

[45] B. Li, N. Madras, and A.D. Sokal. Critical exponents, hyperscaling, and universal amplitude ratios for two- and three-dimensional self-avoiding walks. *J. Statist. Phys.*, **80**:661–754, (1995).

[46] B. MacDonald, D.L. Hunter, K. Kelly, and N. Jan. Self-avoiding walks in two to five dimensions: exact enumerations and series study. *J. Phys. A: Math. Gen.*, **25**:1429–1440, (1992).

[47] B. MacDonald, S. Joseph, D.L. Hunter, L.L. Moseley, N. Jan, and A.J. Guttmann. Self-avoiding walks on the simple cubic lattice. *J. Phys. A: Math. Gen.*, **33**:5973–5983, (2000).

[48] N. Madras and G. Slade. *The Self-Avoiding Walk.* Birkhäuser, Boston, (1993).

[49] N. Madras and A.D. Sokal. The pivot algorithm: A highly efficient Monte Carlo method for the self-avoiding walk. *J. Statist. Phys.*, **50**:109–186, (1988).

[50] B. McKay, W. Myrvold, and J. Nadon. Fast backtracking principles applied to find new cages. In *9th Annual ACM-SIAM Symposium on Discrete Algorithms*, pages 188–191, (1998).

[51] A.M. Nemirovsky, K.F. Freed, T. Ishinabe, and J.F. Douglas. End-to-end distance of a single self-interacting self-avoiding polymer chain: d^{-1} expansion. *Phys. Lett. A*, **162**:469–474, (1992).

[52] A.M. Nemirovsky, K.F. Freed, T. Ishinabe, and J.F. Douglas. Marriage of exact enumeration and $1/d$ expansion methods: Lattice model of dilute polymers. *J. Statist. Phys.*, **67**:1083–1108, (1992).

[53] J. Noonan. New upper bounds on the connective constants of self-avoiding walks. *J. Statist. Phys.*, **91**:871–888, (1998).

[54] A.L. Owczarek and T. Prellberg. Scaling of self-avoiding walks in high dimensions. *J. Phys. A: Math. Gen.*, **34**:5773–5780, (2001).

[55] A. Pelissetto and E. Vicari. Critical phenomena and renormalization-group theory. *Phys. Reports*, **368**:549–727, (2002).

[56] A. Pönitz and P. Tittmann. Improved upper bounds for self-avoiding walks in $\mathbb{Z}^d$. *Electron. J. Combin.*, **7**:Paper R21, (2000).

[57] T. Prellberg. Scaling of self-avoiding walks and self-avoiding trails in three dimensions. *J. Phys. A: Math. Gen.*, **34**:L599–L602, (2001).

[58] G. Slade. Bounds on the self-avoiding-walk connective constant. *Journal of Fourier Analysis and Applications*, Special Issue: Proceedings of the Conference in Honor of Jean-Pierre Kahane (Orsay, June 28 – July 3 1993):525–533, (1995).

[59] G. Slade. *The Lace Expansion and its Applications.* Springer, Berlin, (2006). Lecture Notes in Mathematics Vol. 1879. Ecole d'Eté de Probabilités de Saint–Flour XXXIV–2004.

[60] E. Swierczak. *Numerical problems in statistical mechanics.* PhD thesis, University of Melbourne, (1995).

[61] G. Torrie and S.G. Whittington. Exact enumeration of neighbour-avoiding walks on the tetrahedral and body-centred cubic lattices. *J. Phys. A: Math. Gen.*, **8**:1178–1184, (1975).

[62] J. Zinn-Justin. Analysis of Ising-model critical exponents from high-temperature series expansion. *J. Phys. (France)*, **40**:969–975, (1979).

[63] J. Zinn-Justin. Analysis of high-temperature series of the spin-s Ising model on the body-centred cubic lattice. *J. Phys. (France)*, **42**:783–792, (1981).